İSTANBUL TECHNICAL UNIVERSITY ★ INSTITUTE OF SCIENCE AND TECHNOLOGY

THE EFFECTS of EXTERIOR SHADING DEVICES on FLOW MECHANISMS of BUILDING FAÇADE

M. Sc. Thesis by
Elif ALTUNTAŞ, Mech Eng.

Department : **Mechanical Engineering**

Programme: **Thermo-Fluids**

Supervisor: Dr. Murat ÇAKAN

JANUARY 2007

ISTANBUL TECHNICAL UNIVERSITY ★ INSTITUTE OF SCIENCE AND TECHNOLOGY

THE EFFECTS of EXTERIOR SHADING DEVICES on FLOW MECHANISMS of BUILDING FAÇADE

M. Sc. Thesis by
Elif ALTUNTAŞ, Mech. Eng.

Date of submission : 25 December 2006

Date of defence examination: 29 January 2007

Supervisor (Chairman): Dr. Murat ÇAKAN

Members of the Examining Committee: Dr. Levent KAVURMACIOĞLU

Prof. Dr. Ursula EICKER (S.A.S.)

JANUARY 2007

İSTANBUL TEKNİK ÜNİVERSİTESİ ★ FEN BİLİMLERİ ENSTİTÜSÜ

B İNA YÜZEYLERİNDE GÖLGELEME ELEMANLARININ AKIŞ MEKANİZMALARINA ETKİLERİ

YÜKSEK LİSANS TEZİ

Mak. Müh. Elif ALTUNTAŞ

Tezin Enstitüye Verildiği Tarih : 25 Aralık 2006

Tezin Savunulduğu Tarih : 29 Ocak 2007

Tez Danışmanı :	**Yrd. Doç. Dr. Murat ÇAKAN**
Diğer Jüri Üyeleri	**Yrd. Doç. Dr. Levent KAVURMACIOĞLU**
	Prof.Dr. Ursula EICKER (S.A.S.)

OCAK 2007

FOREWORD

First I would like to express my sincere gratitude to, Dr. Murat ÇAKAN supervisor, for his patience, guidance and encouragement during this research work and in the preparation of this thesis. His wide experiences helped refine and clarify my thoughts.

I would also like to thank Prof. Dr. Ursula EICKER from Stuttgart University of Applied Science, for her guidance, advice and valuable opinions. She helped with her experiences in my thesis study in Stuttgart.

I am grateful to Prof Dr Vildan OK who has helped me about the experimental procedure and research project. Additional thanks go to Dr Levent KAVURMACIOGLU for his valuable advice in CFD simulations.

I also wish to thank my colleagues from Stuttgart University of Applied Sciences.

I wish also acknowledge my research colleagues Ergün ÇEKLİ, Ayse Miray GEMİ, Neslihan TÜRKMENOĞLU, and Evren Öner in particular. Their academic comments and supports helped me to raise the quality of my work.

Special thanks to my great friends, who have stood by me during difficult times.

Finally I would like to thank my parents, Hasan and Şükran Altuntaş, and my brothers and sisters I am heavily indebted to them for endless support.

Elif ALTUNTAŞ

January 2007

TABLE OF CONTENTS

LIST OF ABBREVIATIONS

ABL	: Atmospheric Boundary Layer
CAD	: Computer-aided Design
CIBSE	: The Chartered Institution of Building Services Engineering,
CFD	: Computational Fluid Dynamics
N-S Equations	: Navier-Stokes Equations
PDE	: partial differential equations
Re	: Reynolds Number
RNG	: Renormalization Group k- ε
Lw	: Leewall
Ww	**:**Windwall
Uw	: Upperwall

LIST OF TABLES

LIST OF FIGURES

Page No

LIST OF SYMBOLS

ρ	**:** Density
p	**:** Pressure
u	**:** Instantaneous x-velocity
v	**:** Instantaneous y-velocity
w	**:** Instantaneous z-velocity
τ_{ij}	**:** Viscous stres
δ_{ij}	**:** Kronocker delta function(i=j, δ_{ij} =1 or i ≠ j, δ_{ij} =0)
x_i, x_j	**:** Coordinate variable
q_i	**:** Heat-flux
$\mathbf{d_h}$	**:** Hydraulic diameter
υ	**:** Kinematic viscosity
$\mathbf{y^+}$	**:** Dimensionless wall distance
$\mathbf{U^+}$	**:** Dimensionless velocity
τ_w	**:** Wall shear stress
y	**:** Wall distance
υ_t	**:** Eddy viscosity
k	**:** Kinetic energy
u_τ	**:** Friction velocity
ε	**:** Dissipation rate
U	**:** Time average x-velocity
V	**:** Time average y-velocity
W	**:** Time average z-velocity
u'	**:** Instantaneous deviation from the mean velocity x-axis
v'	**:** Instantaneous deviation from the mean velocity y-axis
w'	**:** Instantaneous deviation from the mean velocity z-axis
$C_\mu, C_{\varepsilon 1}, C_{\varepsilon 2}, \sigma_k, \sigma_\varepsilon$	**:** Turbulence model constants
90_0	**:** Horizontal_closed
90_45	**:** Horizontal_halfclosed
90_90	**:** Horizontal_open
0_0	**:** Vertical_closed
0_45	**:** Vertical_halfclosed
0_90	**:** Vertical_open
45_0	**:** Diagonal_closed
45_45	**:** Diagonal_halfclosed
45_90	**:** Diagonal_open

ABSTRACT

The wind (passive cooling) effect on the building facades can be changed by putting (placing) elements (external shading devices) on the façade. The external shading devices causes pressure drop and make the flow as forced convection. As a result of this, it provides an effective cooling, increasing on internal comfort, and decreasing on energy consumption. A comprehensive modeling of a room in a wind channel with the external shading devices and forced ventilation is proposed here. The modeling is done using the CFD (computational fluid dynamics) approach to assess the air movement within the ventilated façade channel. Two-dimensional airflow is modeled in order to reduce the size of the mathematical model. In this work, the effect of mesh sensibility and turbulence model effects are considered. A parametric study is proposed here, analyzing the impact of two parameters on the airflow development: slat tilt angle and blind position.

ÖZET

Binalardaki rüzgâr etkisi, bina yüzeylerine gölgeleme elemanları konularak değiştirilebilir. Bina yüzeylerine yerleştirilen dış gölgeleme elemanları basınç düşümüne neden olarak akışın zorlamalı akış olmasını sağlar. Bina yüzeylerindeki basınç düşümünün etkisi ile etkin soğutma, iç şartlarda konfor ve enerji tüketiminde düşüm sağlar. Bu etkinin gözlemlenmesi amacıyla yapılan bilgisayarlı analizler rüzgâr tünelinde deneysel olarak analizleri yapılan tek katlı bina modeli temel alınarak yapılmıştır. Modelleme rüzgâr tüneli içindeki bina göz önüne alınarak CFD ile yapılmıştır. Matematiksel modelin boyutunu azaltmak üzere 2 boyutlu akış modellenmiştir. Bu çalışmada, ağ duyarlılığı ve gölgeleme elemanlarının ve levha açılarının etkileri düşünülmüştür. Levha açısının ve gölgeleme elemanının yeri parametre olarak kabul edilerek hava hareketi üzerine parametrik bir çalışma yapılmıştır.

1. INTRODUCTION

1.1 Energy, Buildings and Wind

People spend 90% of their time live and work in buildings. Building Ventilation provides the required amount of fresh air into a building under specified weather and environmental conditions. The process includes supplying air to and removing it from enclosures, disturbing and circulating the air therein, or preventing indoor contamination. Maintaining the indoor thermal comfort for occupants imposes an energy load on buildings.

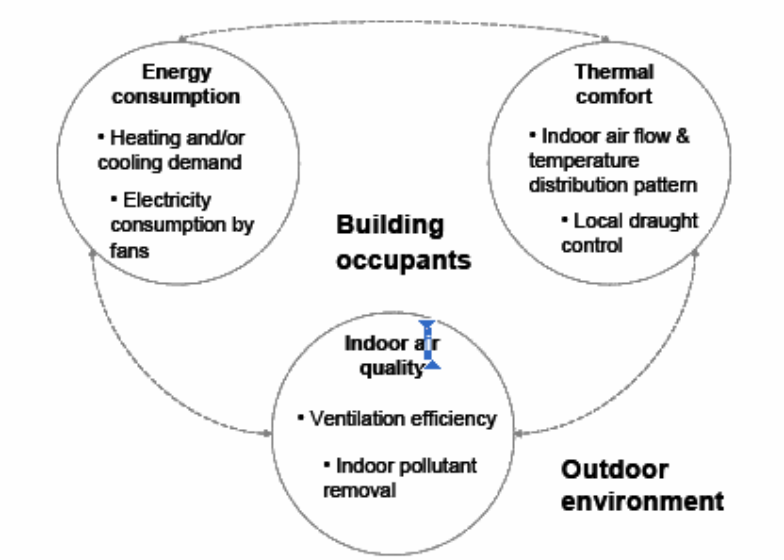

Figure 1.1: The Building- an integrates dynamic system (CIBSE Briefing, 8, 2003)

Energy efficiency in designing and operating buildings can make a big contribution to CO2 emission reduction (depending on Kyoto Protocol to reduce global warming) new low-energy buildings consume 50% less energy than existing buildings (CIBSE Briefing 8, 2003).

Energy efficient design can only be achieved successfully through careful design of built form and services using renewable energy sources (wind, solar energy, etc.) and passive solutions. The natural variation of wind and thermal buoyancy forces continuously changes the airflow into a naturally ventilated building. In particular, the air flow through an opening, either purpose provided or adventitious, depends on

the pressure difference between the sides of the opening, as well as on the resistance opposed to the air flow by the opening itself; the latter is a function of opening shape and dimension. The pressure difference is produced by wind and buoyancy forces, several studies have been performed in order to better understand the interaction between these two driving forces. Allocca et al. showed that, under certain circumstances natural ventilation and are limited to relatively simple geometry. CFD techniques offer detailed information about indoor flow patterns, air movement, and temperature and local, the wind effect might not be beneficial, as it may reduce the ventilation rate provided by buoyancy forces alone.

Using exterior shading devices on the building facades is a method for controlling the natural ventilation inside the building. They used mainly in tropical climates to reduce the solar gains and cause the venture effect for the view of airflow phenomena.

In general three approaches are available to study natural ventilation: empirical/semi-empirical, experimental, and computational. The first two approaches do not provide sufficient information on draught distribution in buildings, so that it has unique advantages as an efficient and cost effective tool for optimum design in a complex built environment.

Recent development of CFD techniques in natural ventilation studies has been applied to modeling external flow around buildings and indoor thermal comfort simulation separately (Cook et al., 2003; Chen, 2004); simulating the combined indoor and outdoor airflows through large openings in wind tunnel models (Jiang et al., 2003); in a full-scale building placed in wind tunnel (Nishiawa et al., 2003) and in full-scale buildings located in the natural environment (Straw, 2000).

1.2 Research Objectives

The main aim of this project is to understand the airflow mechanisms around the exterior shading devices and inside the building depending on the different slat tilt angles and the position of the exterior shading devices. A commercial CFD program, FLUENT6.2 is used for this project. The effects of grid sensitivity, turbulence models, and position and slat angles of shading devices are analyzed.

1.3 Structure of the Thesis

Chapter 2 contains a brief review of the building ventilation systems, wind effects on the buildings, atmospheric boundary layer and shading devices.

Chapter 3 explains the Computational Fluid Dynamics, the methodology of the used commercial CFD programs, Gambit and Fluent, and the used Governing Equations for this Program. In this chapter, turbulence phenomena and modeling is explained.

Chapter 4 identifies the research model. The experimental method and numerical method of the project and the used definitions and boundary conditions are explained.

Chapter 5 focuses on the results of the numerical method, which are grid sensitivityand effects of shading devices. In this section, the comparison of the numerical results of all cases are shown.

In Chapter 6 includes the conclusion and the recommendation for the future work.

2. LITERATURE REVIEW

Building ventilation plays an important role in providing good air quality and thermal comfort for the occupants. Ventilation is achieved by;

- Natural Ventilation
- Mechanical Ventilation
- Hybrid ventilation

Natural ventilation systems rely on natural driving forces, such as wind and temperature difference between a building and its environment, to supply fresh air to building interiors (BSI, 1991).

Mechanical ventilation makes use of electrically powered fans or more complex ducting and control systems to supply and/or extract air to and from the building (CIBSE AM 10, 1997).

Hybrid ventilation systems provide a comfortable internal environment using both natural ventilation and mechanical ventilation systems (Heiselberg, 1999). The main aim of hybrid systems is to optimize the most effective and energy efficient systems by using natural and mechanical ventilation systems.

2.1 Natural Ventilation

This section gives an overview of natural ventilation in commercial buildings and its potential advantages and issues to overcome.

2.1.1 Introduction to Natural Ventilation

Ventilation, whether mechanical or natural, may be used for:

• Air Quality Control: to control building air quality, by diluting internally-generated air contaminants with cleaner outdoor air,

• Direct Advective Cooling: to directly cool building interiors by replacing or diluting warm indoor air with cooler outdoor air when conditions are favorable,

• Direct Personal Cooling: to directly cool building occupants by directing cool outdoor air over building occupants at sufficient velocity to enhance convective transport of heat and moisture from the occupants, and

• Indirect Night Cooling: to indirectly cool building interiors by pre-cooling thermally massive components of the building fabric or a thermal storage system with cool night time outdoor air.

While these four distinct purposes must be kept in mind when designing a natural ventilation system, direct advective and personal cooling are reasonably achieved in an integrated manner by a properly designed direct cooling strategy. Consequently, just three purposes are most often noted in the literature–air quality control, direct cooling, and indirect cooling.

Natural ventilation may be defined as ventilation provided by thermal, wind or diffusion effects through doors, windows, or other intentional openings in the building as opposed to mechanical ventilation that is ventilation provided by mechanically powered equipment such as motor-driven fans and blowers. Although some in the U.S. may think of natural ventilation as simply meaning operable windows, natural ventilation technology has been advanced in recent years in Europe and elsewhere.

The variety and diversity of purpose-provided natural ventilations systems that have been proposed in recent years is staggering. Hybrid variations of many of these systems, wherein mechanical devices are added to enhance system performance and control, add yet another level of complication. Nevertheless, these systems are invariably conceived as variants of three fundamental approaches to natural ventilation:

• Wind-driven cross ventilation

• Buoyancy-driven stack ventilation, and

• Single-sided ventilation.

2.1.2 Wind-Driven Cross Ventilation

Wind-driven cross ventilation occurs via ventilation openings on opposite sides of an enclosed space. Figure 2-1 shows a schematic of cross ventilation serving a multi-room building, referred to here as global cross ventilation. The building floor plan depth in the direction of the ventilation flow must be limited to effectively remove heat and pollutants from the space by typical driving forces. A significant difference in wind pressure between the inlet and outlet openings and a minimal internal resistance to flow are needed to ensure sufficient ventilation flow. The ventilation openings are typically windows.

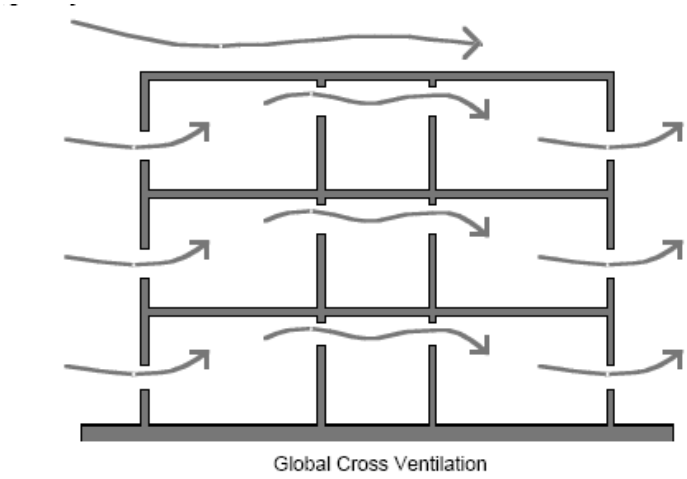

Figure 2.1: Schematic of wind driven cross ventilation

2.1.3 Buoyancy-Driven Stack Ventilation

Buoyancy-driven stack ventilation relies on density differences to draw cool, outdoor air in at low ventilation openings and exhaust warm, indoor air at higher ventilation openings. Figure 2.2 shows a schematic of stack ventilation for a multi-room building. A chimney or atrium is frequently used to generate sufficient buoyancy forces to achieve the needed flow. However, even the smallest wind will induce pressure distributions on the building envelope that will also act to drive airflow.

Indeed, wind effects may well be more important than buoyancy effects in stack ventilation schemes, thus the successful design will seek ways to make full advantage of both.

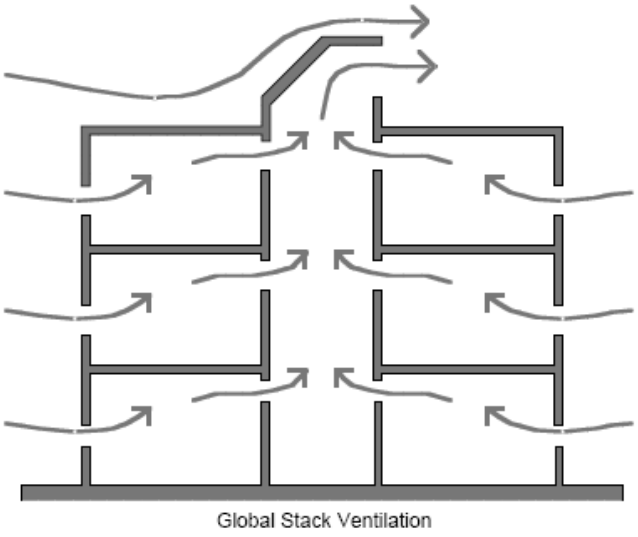

Figure 2.2: Buoyancy-driven stack ventilation

2.1.4 Single-Sided Ventilation

Single-sided ventilation typically serves single rooms and thus provides a local ventilation solution. Figure 2-3 shows a schematic of single-sided ventilation in a multi-room building.

Ventilation airflow in this case is driven by room-scale buoyancy effects, small differences in envelope wind pressures, and/or turbulence. Consequently, driving forces for single-sided ventilation tend to be relatively small and highly variable. Compared to the other alternatives, single-sided ventilation offers the least attractive natural ventilation solution but, nevertheless, a solution that can serve individual offices.

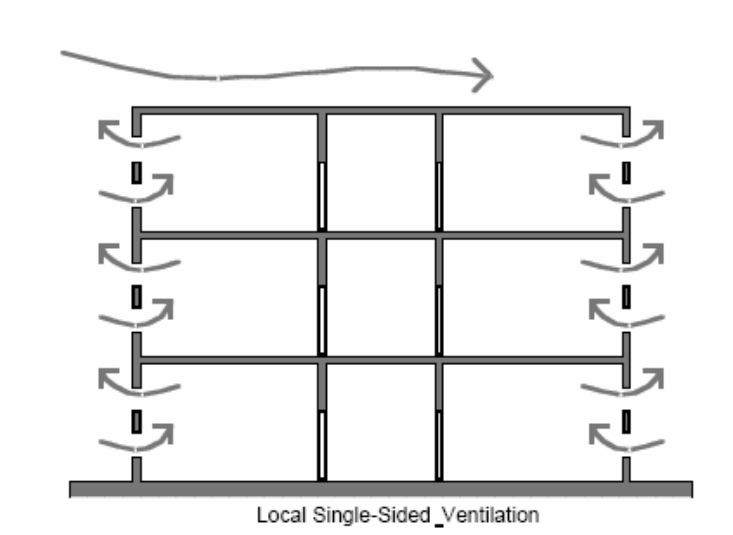

Figure 2.3: Schematic of single sided ventilation

2.2 Wind Engineering, Atmospheric Boundary Layer (ABL), and Effects on Building

Wind is the term used for air in motion and is usually applied to the natural horizontal motion of the atmosphere. The horizontal motion of air, particularly the gradual retardation of wind speed and the high turbulence that occurs near the ground surface, are of importance in building engineering. Wind can be a friend of a building because it can naturally ventilate the building, providing a comfortable and healthy indoor environment, as well as saving energy. Natural ventilation can be used for cooling in the spring and autumn for a moderate climate (e.g., Nashville, TN); the spring for a hot and dry climate (e.g. Phoenix, AZ); the summer for a cold climate (e.g. Portland, ME); and the spring and summer for a mild climate (e.g. Seattle, WA). Natural ventilation can also be used to cool environments in a hot and humid climate during some of the year (e.g. New Orleans, LA) (Lechner, 2000).

Conventional design approaches often ignore opportunities for innovations with wind that could condition buildings at a lower cost, while providing higher air quality and an acceptable thermal comfort level, by means of passive cooling or natural ventilation. On the other hand, wind can be an enemy to a building when it causes discomfort to pedestrians-usually as a result of high wind speed around the building. Table 2.1 summarizes the effect of wind on the people.

Table 2.1: Wind effect on people (Bottema, 1980)

Beaufort no.	Description	Wind speed(m/s)	Wind effect
2	Light breeze	1.6-3.3	Wind felt on face
3	Gentle breeze	3.4-5.4	Hair disturbed; clothing flaps; newspaper difficult to read
4	Moderate breeze	5.5-7.9	Raises dust and lose paper; hair disarranged
5	Fresh breeze	8.0-10.7	Wind force felt by body, possible stumbling when entering a windy zone
6	Strong breeze	10.8-13.8	Umbrellas used with difficulty, hair blown straight, difficult in walking steadily, wind noise on ears unpleasant
7	Near gale	13.9-17.1	Inconvenience felt when walking
8	Gale	17.2-20.7	Generally impedes progress, great difficulty with balance in gusts
9	Strong gale	20.8-24.4	People blown over

The assessment of wind effects on building structures requires knowledge of the complex interactions that involve meteorology, aerodynamics and building structures. The great majority of buildings and structures in the field of wind engineering are considered as bluff bodies. A body is referred to as bluff, when the aerodynamic flow streamlines are detached from the surface of the body. This is encountered with the formation of separated flow around the body, creating a wide trailing turbulent wake (Cook, 1985).

2.2.1 Characteristics of Wind

The flow of wind is not steady and fluctuates in a random fashion. Because of this, wind loads imposed on buildings are studied statistically. The wind flow is complex depending on the flow situations, which arise from the interaction of wind with

structures. Simplifications are made to arrive at design wind loads by distinguishing the following characteristics:

- Variation of wind velocity with height
- Wind Turbulence
- Statistical probability
- Vortex shedding phenomena
- Dynamic nature of wind-structure interaction

2.2.2 Distribution of Pressures and Suctions

When air flows around edges of a structure, the resulting pressures at the corners are much in excess of the pressures on the center of elevation. This has been evidence by damage caused to corner windows, eave and ridge tiles etc, in windstorms. Wind tunnel studies conducted on scale models of buildings indicate that three distinct pressure areas develop around a building. These are shown in Figure 2.4.

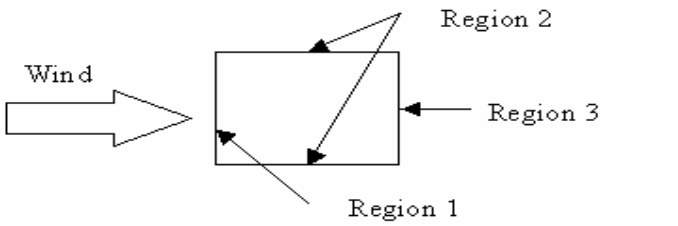

Figure 2.4: Pressure zones around a building

1. Positive pressure zone on the upstream Face (Region1).
2. Negative pressure zones at the upstream corners (Regions 2).
3. Negative pressure zone on the downstream face (Region 3).

2.2.3 Atmospheric Boundary Layer

The atmospheric boundary layer (ABL) is the layer of turbulent flow between the Earth's surface and undisturbed wind, with thickness is determined by the gradient height at which surface friction of the ground no longer affects the general flow of wind. The bottom 5 to 10% of the ABL is considered as the roughness sub-layer. This layer is affected by the frictional forces exerted by the ground, i.e. fences, trees, buildings, etc. The average wind speed increases with the height above the ground, while the intensity of the turbulence or gusting decreases. The difference in terrain

conditions directly affects the magnitude of the frictional force and causes the mean wind speed variations.

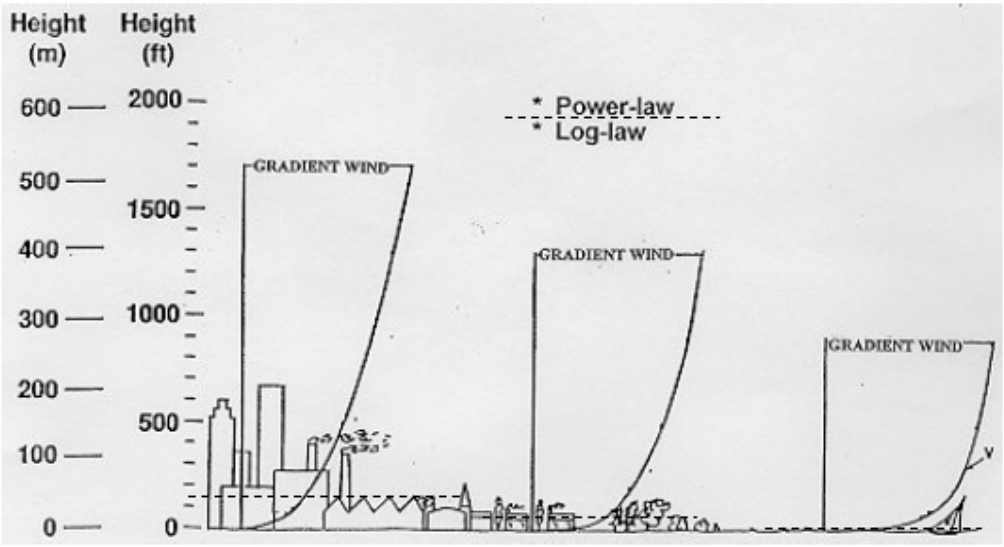

Figure 2.5: Wind speed variations with height and terrain conditions (Source: www.wind.ttu.edu)

Most flows in nature and engineering practice are turbulent. In the ABL, the complex terrain increases the roughness of the surface and therefore increases the turbulence. Turbulent flows are unsteady and contain fluctuations that are chaotic in space and time. This affects the airflow around the buildings.

2.3 Shading Devices

Shading devices are used for preventing high solar gains and controlling the wind effect on cross ventilation. Increasing the performance of natural ventilation system, the position and the type of the shading devices should be considered. There are three main solar control methods that are;

1.Vegetation

2.Interior Shading Devices

3.Exterior shading Devices

Vegetation is a natural and beautiful way to shade buildings (especially residential) and block the sun. A well-placed tree, bush or vine can deliver effective shade and add aesthetic value to your property as well as reduce summer air conditioning costs.

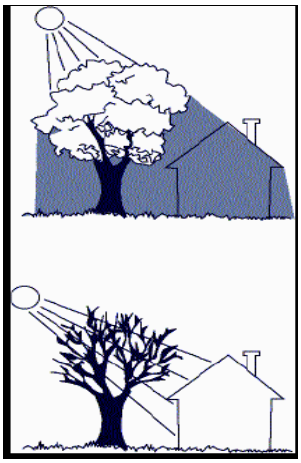

Figure 2.6: Vegetation with a tree

Interior shading devices such as curtains and venetian blinds can shade rooms from direct light and be adjusted to allow in daylight or eliminate solar radiation. The added benefit of venetian blinds is that they can be adjusted to reflect light up to the ceiling, brightening the room without heat gain or having to turn on the lights.

Exterior shading devices are generally more effective in decreasing heat buildup because they block, absorb or reflect solar heat before it gets into your windows. Exterior shading devices include awnings, louvers, shutters, rolling shutters and shades and solar screens.

2.3.1 Exterior Shading Devices

External shading devices have been utilized very extensively in energy-efficient building design strategies to reduce the amount of solar radiation entering into the buildings. They affect the availability of day-lighting and natural ventilation performance. In term of day-lighting there are two effects i.e. avoiding glare problem and reduction of light intensity. From the natural ventilation effect the shading devices can be used as wind catcher. However, it must be designed and located in the right place, which otherwise can become a barrier to wind flow (wind breaker).

The design of effective shading devices will depend on the solar orientation of a particular building facade. For example, simple fixed overhangs are very effective at shading south-facing windows in the summer when sun angles are high. However, the same horizontal device is ineffective at blocking low afternoon sun from entering west-facing windows during peak heat gain periods in the summer.

External shading is a general technique that it can be accomplished with many different types of hardware or architectural features. Shading may be fixed or movable. The most used external shading devices and best orientations are summarized in Table 2.2.

Table 2.2: Exterior Shading Devices (Lechner, 2000)

1)Overhang - Horizontal Panel	2)Overhang- Horizontal louvers in horizontal plane	3)Overhang- Horizontal louvers in vertical plane	4)Overhang-Vertical panel
			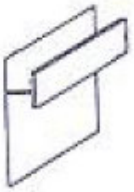
• **Best orientation**: South, East and West • **Comments** Traps hot air Can be loaded by snow or wind	• **Best orientation:** South, East and West • **Comments** Free air movement Snow or wind load is small	• **Best orientation:** South, East and West • **Comments** Reduces length of overhang, View restricted	• **Best orientation:** South, East and West • **Comments** Free air movement No snow load View restricted
5)Vertical fin	**6)Vertical fin slanted**	**7)Eggerate**	**8)Eggerate with slanted fins**
			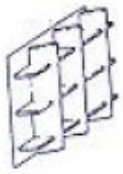
• **Best orientation**: East, West and North • **Comments** Restricts view For north facades in hot climates only	• **Best orientation:** East, West • **Comments** Slant toward north Restricts view significantly	• **Best orientation:** East, West • **Comments** For very hot climates View very restricted Traps hot air	• **Best orientation:** East, West • **Comments** Slant toward north View very restricted Traps hot air For very hot climates

2.4 Analysis and Design Tools

Suitable and valid analytical method of natural ventilation system would give architects and engineers the necessary confidence in ventilation system performance, which is also decisive factor for choice of system design.

Most of the publications (Liddament, 1991; Allard, 1998; Chen and Xu, 1998; Li et al., 1998; Hunt and Linden, 1999; Straw, 2000; Etheridege, 2002; Jiang et al., 2003) cover the theoretical approaches, laboratory experiments, field studies, and numerical/computational simulations of the performance of natural ventilation systems. The advantages and disadvantages of the various methods are listed in Table 2.3.

Table 2.3: Advantages and disadvantages of theoretical and experimental methods (Gan,1999)

Approach		Advantages	Disadvantages
Theoretical	Envelope flow Models	1.Simple, usually in formula or graphical form	1. Restricted to simple geometry 2. Assumptions are needed about the details of the flow to obtain simplified flow equations for bulk flow
	CFD Flows	1.Predict flow field in details 2. Resolve flow feature development with time 3.Greater flexibility	1. Numerical truncation errors 2. Boundary condition problems 3. Assumptions about turbulence structure and near wall treatment 4. Computer costs 5. Experienced user costs
Experimental		1. Capable of being most realistic	1. Equipment required 2. Scaling problems 3. Tunnel corrections 4. Measuring difficulties 5. Operating Costs

3. COMPUTATIONAL FLUID DYNAMICS

Computational Fluid Dynamics (CFD) is a computational technology and method that enables to study complex fluid flow, heat transfer, and chemical reaction problems. It solves mathematical equations which represent physical laws, i.e. conservation of mass, momentum, energy, species… Using CFD software, it is possible to build a 'virtual prototype' of the system or device that is wished to analyze and then apply real-world physics and chemistry to the model, and the software will provide with images and data, which predict the performance of that design.

CFD divides a flow area into a large number of cells or control volumes, collectively referred to as the “mesh” or “grid”. In each of the cells, the Navier-Stokes Equations, i.e. the partial differential equations that describe fluid flow are rewritten algebraically, to relate such variables as pressure, velocity and temperature in neighboring cells.

There are three main benefits of CFD which can be summarized as below (FLUENT6.2, 2006):

1. Insight: If there is a device or system design which is difficult to prototype or test through experimentation, CFD analysis enables you to virtually crawl inside your design and see how it performs. There are many phenomena that can be solved through CFD, which wouldn't be visible through any other means. CFD gives the designer a deeper insight into the designs.

2. Foresight: CFD is a tool for predicting what will happen under a given set of circumstances, it can quickly answer many 'what if?' questions. It can be predicted how the design will perform, and test many variations until is arrived at an optimal result. All of this can be done before physical prototyping and testing.

3. Efficiency: The foresight, which is gained from CFD, helps to design better and faster, save money, meet environmental regulations and ensure industry compliance. Equipment improvements are built and installed with minimal downtime. CFD is a tool for compressing the design and development cycle allowing for rapid prototyping.

There are essentially three stages to every CFD simulation process: preprocessing, solving and post-processing.

1. Preprocessing: It is the first step in building and analyzing a flow model. It includes building the model within a computer-aided design (CAD) package, creating and applying a suitable computational mesh, and entering the flow boundary conditions and fluid materials properties.

2. Solving: The CFD solver does the flow calculations and produces the results. Most of the CFD programs provide the broadest range of rigorous physical models that have been validated against industrial scale applications, so it can be accurately simulated real-world conditions, including:

- Multiphase flows
- Reacting flows
- Rotating equipment
- Moving and deforming objects
- Turbulence
- Radiation
- Acoustics, and
- Dynamic meshing

3. Post-processing: This is the final step in CFD analysis, and it involves the organization and interpretation of the predicted flow data and the production of CFD images and animations.

The procedure of solution method in Gambit and FLUENT could be seen in Table 3.1 easily. Geometry, physics and Mesh parts are drawn generally in Gambit. Solve, Reports and Post-Processing parts are solved generally in FLUENT. However there is not certain distinction between them.

Table 3.1: Schema of the CFD

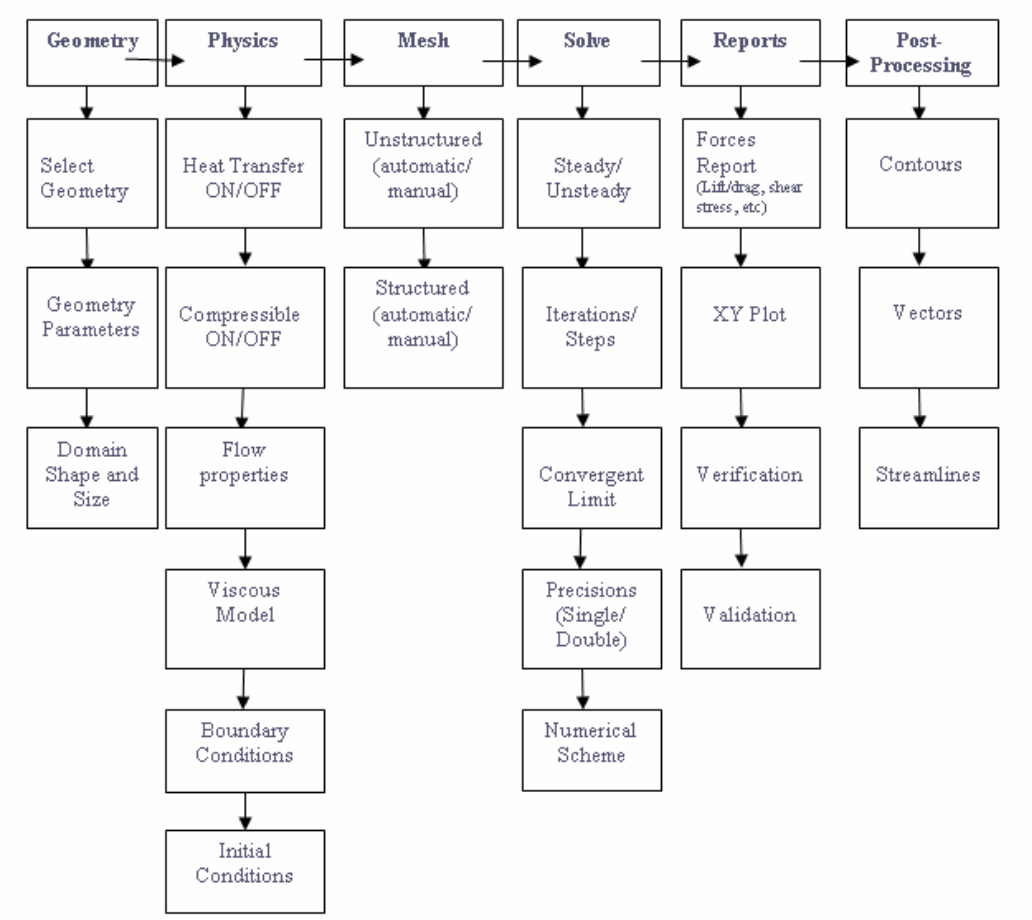

3.1 Gambit

Gambit is an integrated preprocessor for CFD analysis. It can be used to build geometry and to generate a mesh, or to import a geometry created by a third-party CAD/CAE package. It is also Fluent's geometry and mesh generation software. GAMBIT's single interface for geometry creation and meshing brings together most of Fluent's preprocessing technologies in one environment. Advanced tools for journaling let the user edit and conveniently replay model-building sessions for parametric studies. GAMBIT's combination of CAD interoperability, geometry cleanup, decomposition and meshing tools results in one of the easiest, fastest, and most straightforward preprocessing paths from CAD to quality CFD meshes. GAMBIT's unique curvature and proximity based "size function" produces a correct and smooth CFD-type mesh throughout the model. The interface of Gambit is shown in Figure 3.1.

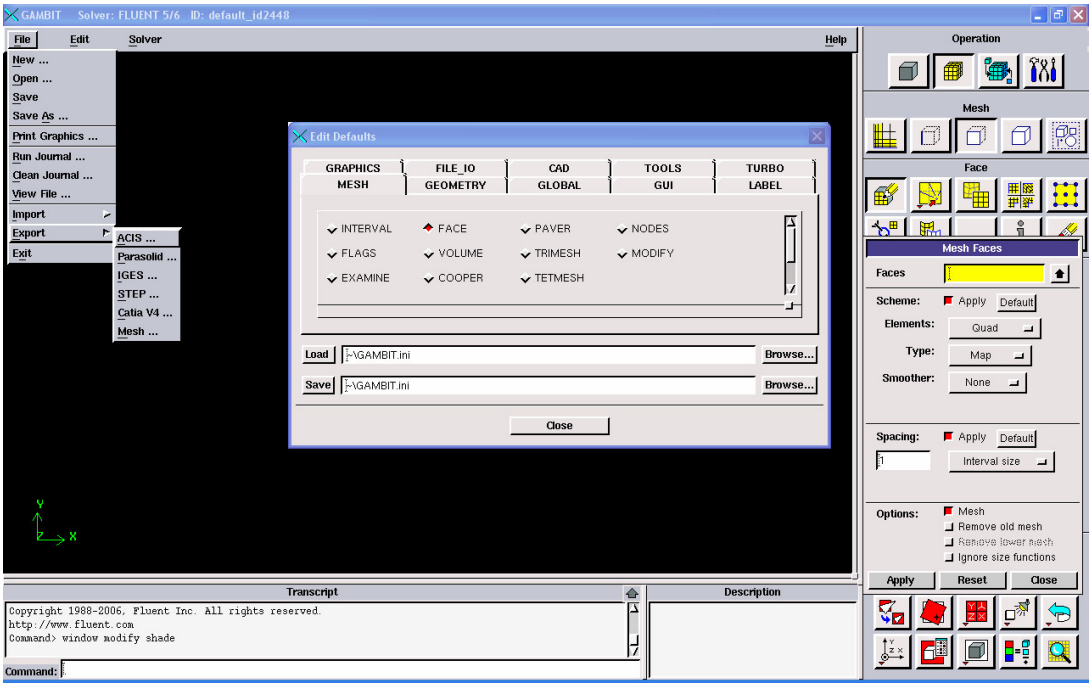

Figure 3.1: Gambit

The case study could be modeled in 2/3-D, meshed, and the boundary conditions could be defined. The default parameters for the case, i.e. mesh, geometry, global, can be arranged by the methodology and solution definitions of the case study. Detailed information about Gambit can be found in FLUENT's user services.

3.2 Fluent

Fluent is a commercial CFD program, which is based on finite volume method and is a general-purpose package for modeling fluid flow and heat transfer. The Fluent CFD code has extensive interactivity, so it is possible to make changes to the analysis at any time during the process. This saves time and enables to refine the designs more efficiently. It is easy to customize physics and interface functions to your specific needs.

The Fluent solver has repeatedly proven to be fast and reliable for a wide range of CFD applications. The speed to solution is faster because the suite of software enables to stay within one interface from geometry building through the solution process, to post processing and final output. FLUENT's performance has been tried and proven on a variety of multi-platform clusters. The interface of of FLUENT is shown in Figure 3.2.

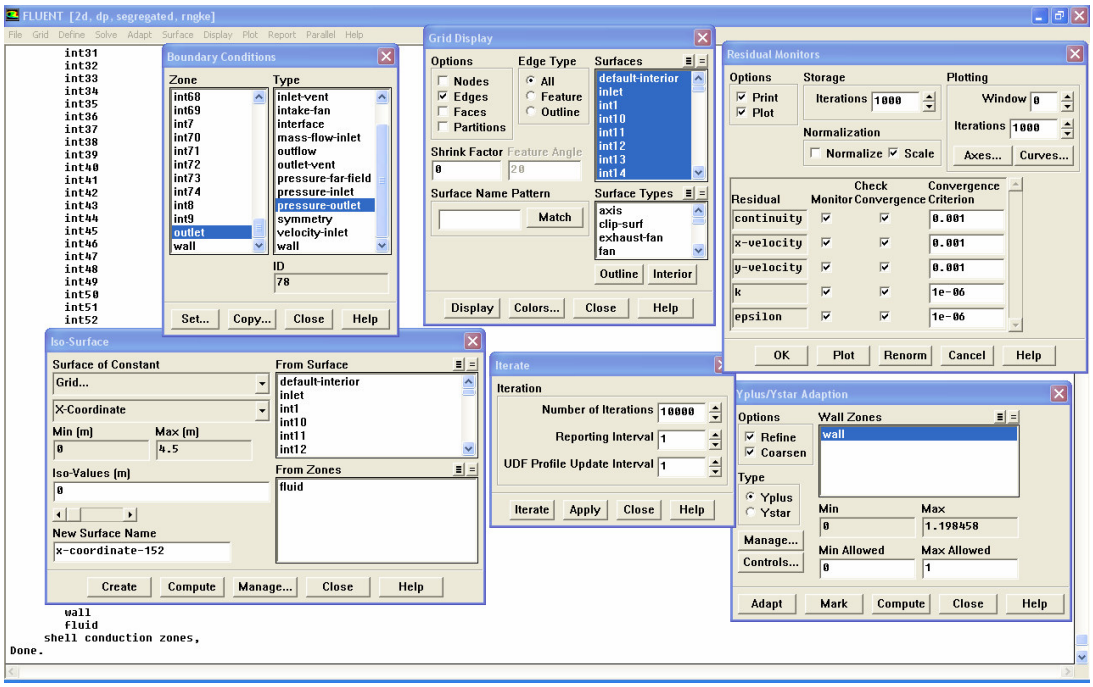

Figure 3.2: Fluent

Fluent's software products include full post-processing capabilities. The post-processing tools enable the user to provide several levels of reporting. Quantitative data analysis can be as sophisticated as it requires.

Main features of the Fluent are (FLUENT, 2006):

- Computer program for modeling fluid flow and heat transfer in complex geometries.
- Provides complete mesh flexibility, solving flow problems with unstructured meshes that can be generated about complex geometries with relative ease.
- Supported mesh types include 2D triangular / quadrilateral, 3D tetrahedral / hexahedral / pyramid / wedge, and mixed (hybrid) meshes.
- Allows users to refine or coarsen their grid based on the flow solution.
- Written in the C computer language and makes full use of the flexibility and power offered by the language.
- True dynamic memory allocation, efficient data structures, and flexible solver control are all made possible.
- Uses a client/server architecture, which allows it to run as separate simultaneous processes on client desktop workstations and powerful compute servers, for efficient execution, interactive control, and complete flexibility of machine or operating system type.

A combined solution for Gambit and Fluent can be obtained by following steps:

1. Creation of the geometry in GAMBIT
2. Mesh geometry in GAMBIT
3. Set boundary types in GAMBIT
4. Set Up Problem in FLUENT
5. Solve
6. Analyze Results
7. Refine Mesh

Applying these steps, there will be an accurate and sensible solution.

3.3 Governing Equations

The fundamental governing equations of fluid dynamics, i.e. the continuity, momentum, and energy equations are the mathematical statements of three fundamental physical principles, which can be regarded as follows:

- Conservation of mass (Continuity Equation)
- Newton's Second Law (Momentum Equation)
- Conservation of Energy (first law of thermodynamics)

Utilizing the finite volume method, the equation for the conservation of mass is discretized by means of a mass balance for a finite volume. Thus for a steady incompressible fluid with uniform temperature, the incoming mass flow is equal to the outgoing mass flow.

By applying Newton's Second Law of Motion, the relationship between the forces on a control volume of fluid and the acceleration of the fluid gives an expression for the conservation of momentum.

The First Law of Thermodynamics states that energy is conserved in fluid. It ensures the rate of change of energy of the fluid particle and the net rate of heat addition to the fluid and the rate of increase of energy due to sources (Verseg and Malalasekera, 1995). This would therefore allow the definitions of changes in fluid temperature within a control volume.

These fundamental principles can be expressed in terms of a set of partial differential equations (PDEs) and in solving these equations the velocity, temperature and pressure are predicted throughout the flow field.

$$\frac{\partial \rho}{\partial t} + \frac{\partial}{\partial x_i}(\rho u_i) = 0 \qquad \textbf{(3.1)}$$

$$\frac{\partial}{\partial t}(\rho u_i) + \frac{\partial}{\partial x_i}(\rho u_i u_j + \delta_{ij} - \tau_{ij}) = 0 \qquad \textbf{(3.2)}$$

$$\frac{\partial}{\partial t}(\rho e_{tot}) + \frac{\partial}{\partial x_i}(\rho_i e_{tot} + u_i p + q_i - u_i \tau_{ij}) = 0 \qquad \textbf{(3.3)}$$

$$f(p, \rho, T) = 0 \qquad \textbf{(3.4)}$$

where

ρ density

p pressure

u instantaneous velocity

τ_{ij} viscous stress

δ_{ij} Kronocker delta function (i=j, δ_{ij} =1 or i ≠ j, δ_{ij} =0)

x_i, x_j coordinate variable

T thermodynamic temperature

e_{tot} total-energy is defined by $e_{tot} = e + u_i u_i / 2$

q_i heat-flux

In the flow of compressible fluids, the equation of state Eq-4 provides the linkage amongst the energy equation, mass conservation and the momentum equations. The functional form of state depends on the nature of the fluid.

The flow of constant-property Newtonian fluids is governed by the Navier-Stokes (N-S) equations together with the mass conservation equation only. Liquids and gases flowing at low speeds behave as incompressible fluids.

The simplified N-S equations for an incompressible Newtonian fluid in the notation of Cartesian tensors can be written as:

$$\frac{\partial u_i}{\partial t} + \partial u_j \frac{\partial u_i}{\partial x_j} = -\frac{1}{\rho}\frac{\partial p}{\partial x_i} + \upsilon \frac{\partial^2 u_i}{\partial x_j^2} \qquad \textbf{(3.5)}$$

where $\upsilon \equiv \frac{\mu}{\rho}$ is the kinematic viscosity

Considering the hypothetical case of an ideal (inviscid) fluid, the isotropic stress tensor is

$$\tau_{ij} = -P\delta_{ij} \qquad \textbf{(3.6)}$$

The physical interpretation of the eddy Reynolds stresses is the effect of turbulent transport of momentum across the main flow direction, which influences the flow in the same way as increased shear stress. The stress tensor is given by:

$$\tau_{ij} = -P\delta_{ij} + \mu\left(\frac{\partial U_i}{\partial x_j} + \frac{\partial U_j}{\partial x_i}\right) \qquad \textbf{(3.7)}$$

This plays an important role in the numerical treatment of turbulence.

The source term contains any extra phenomena taking place in the system, such as the application of wall functions, gravitational and pressure-effects.

3.4 Turbulence

Turbulence is the state of fluid motion, which is characterized by apparently random and chaotic three-dimensional vorticity. When turbulence is present, it usually dominates all other flow phenomena and results in increased energy dissipation, mixing, heat transfer, and drag.

There is no exact definition on turbulent flow, but it has a number of characteristic features (Tennekes & Lumley, 1972) such as:

1. Irregularity: Turbulent flow is irregular, random and chaotic. The flow consists of a spectrum of different scales (eddy sizes) where largest eddies are of the order of the flow geometry (i.e. boundary layer thickness, jet width, etc). At the other end of the spectra there has the smallest eddies which are by viscous forces (stresses) dissipated

into internal energy. Even though turbulence is chaotic it is deterministic and is described by the Navier-Stokes equations.

2. Diffusivity: In turbulent flow the diffusivity increases. This means that the spreading rate of boundary layers, jets, etc. increases as the flow becomes turbulent. The turbulence increases the exchange of momentum in e.g. boundary layers and reduces or delays thereby separation at bluff bodies such as cylinders, airfoils and cars. The increased diffusivity also increases the resistance (wall friction) in internal flows such as in channels and pipes.

3. Large Reynolds Numbers: Turbulent flow occurs at high Reynolds number. For example, the transition to turbulent flow in pipes occurs that Re_D~2300, and in boundary layers at Re_D~100000.

4. Three Dimensional: Turbulent flow is always three-dimensional. However, when the equations are time averaged it can be treated the flow as two-dimensional.

5. Dissipation: Turbulent flow is dissipative, which means that kinetic energy in the small (dissipative) eddies are transformed into internal energy. The small eddies receive the kinetic energy from slightly larger eddies. The slightly larger eddies receive their energy from even larger eddies and so on. The largest eddies extract their energy from the mean flow. This process of transferred energy from the largest turbulent scales (eddies) to the smallest is called cascade process.

6. Continuum: Even though there are small turbulent scales in the flow they are much larger than the molecular scale and it can be treated the flow as a continuum.

In turbulent flow, the flow and fluid variables vary with time and position. The time-averaged velocity is the man factor for describing bulk flow, but does not precisely account for the instantaneous behavior. The instantaneous quantities can be expressed as the summation of the average value and their instantaneous deviation from the average.

The instantaneous velocity components in x-, y-, z- Cartesian coordinates are then:

$$u = U + u' \qquad v = V + v' \qquad w = W + w' \tag{3.8}$$

Where capital letter denotes the time average and prime represents the instantaneous deviation from the mean.

Turbulence is a decisive practical phenomenon that has therefore been extensively studied in the context of its applications by engineers and applied scientists. The outcomes of these studies have also been combined with modern numerical computing techniques.

Table 3.2: Hierarchy of turbulence models (Blazek, 2001)

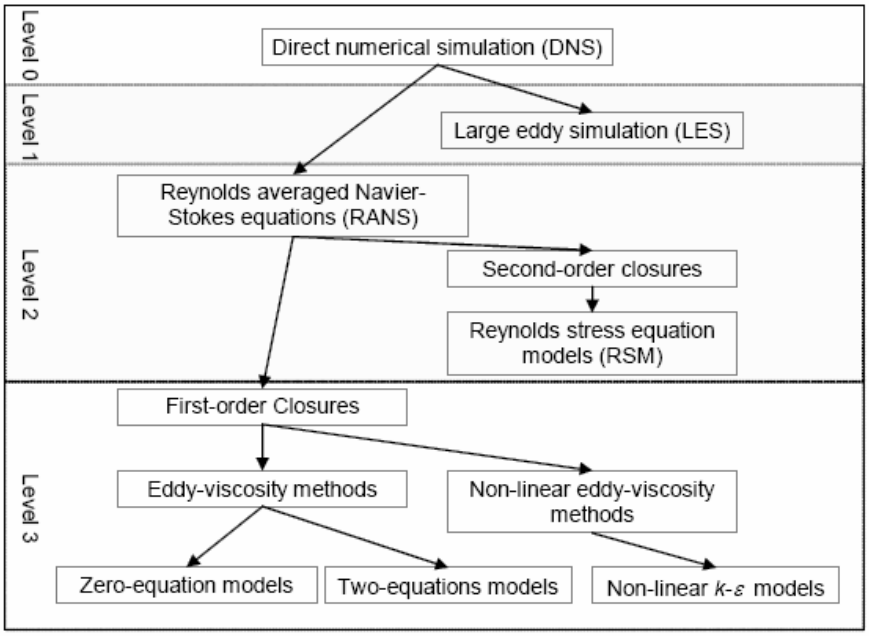

In Table 3.2., different types of turbulence models have been listed in decreasing increasing order of complexity, ability to model the turbulence, and cost in terms of computational work (CPU time).

3.4.1 Standard k-ε Turbulence Model

As cited in Launder and Spalding (1974), two-equation k- ε model is unarguably the most widely used and validated model employed for turbulent fluid dynamics to date. The extensive use of the model has highlighted both the capabilities and shortcomings of the model.

The model has achieved notable success when dealing with thin shear layers and recirculating flows without the need for case-by-case modification of the model constants. Also success of the model is noted for confined flows where the normal Reynolds stresses are relatively unimportant compared to the Reynolds shear stresses, which are of utmost importance.

The model is favored for industrial applications due to its relatively low computational expense and generally better numerical stability than more complex turbulence models such as the Differential Stress Equation Model (DSM) introduced by Launder and Spalding (1974).

The formulation for Launder and Spalding's turbulence model consists of two transport equations, one equation to describe the kinetic energy of turbulence and a second related to the rate of turbulent dissipation.

The k-e model is one of the most common turbulence models. It is a two-equation model that means it includes two extra transport equations to represent the turbulent properties of the flow. This allows a two-equation model to account for history effects like convection and diffusion of turbulent energy. The first transported variable is turbulent kinetic energy, k. The second transported variable in this case is the turbulent dissipation, ε. It is the variable that determines the scale of the turbulence, whereas the first variable, k, determines the energy in the turbulence.

Transport equations for standard k- ε model

For k:

$$\frac{\partial k}{\partial t} + U_i \frac{\partial k}{\partial x_i} = \frac{\partial}{\partial x_i}\left(\frac{\upsilon_t}{\sigma_k}\frac{\partial k}{\partial x_i}\right) + v_t \frac{\partial U_i}{\partial x_j}\left(\frac{\partial U_i}{\partial x_j} + \frac{\partial U_j}{\partial x_i}\right) - \varepsilon \qquad \textbf{(3.9)}$$

For dissipation ε:

$$\frac{\partial \varepsilon}{\partial t} + U_i \frac{\partial \varepsilon}{\partial x_i} = \frac{\partial}{\partial x_i}\left(\frac{\upsilon_t}{\sigma_\varepsilon}\frac{\partial \varepsilon}{\partial x_i}\right) + C_{\varepsilon 1} v_t \frac{\varepsilon}{k}\frac{\partial U_i}{\partial x_j}\left(\frac{\partial U_i}{\partial x_j} + \frac{\partial U_j}{\partial x_i}\right) - C_{\varepsilon 2}\frac{\varepsilon^2}{k} \qquad \textbf{(3.10)}$$

The isotropic eddy viscosity is modeled as:

$$\upsilon_t = C_\mu \frac{k^2}{\varepsilon} \qquad \textbf{(3.11)}$$

where C_μ=0.09, $C_{\varepsilon 1}$=1.44, $C_{\varepsilon 2}$= 1.92, σ_k=1.0 and σ_ε=1.3

The most widely used engineering turbulence model for industrial applications Robust and reasonably accurate; it has many sub-models for compressibility, buoyancy, and combustion etc. This turbulence model performs poorly for flows with strong separation, large streamline curvature, and high-pressure gradient.

3.4.2 RNG k- ε Model

Constants in the k- ε equations are derived using the Renormalization Group method.

RNG's sub-models include:

- Differential viscosity model to account for low-Re effects
- Analytically derived algebraic formula for turbulent Prandtl/Schmidt number
- Swirl modification

RNG k- ε model performs better than SKE for more complex shear flows, and flows with high strain rates, swirl, and separation.

3.4.3 Wall Functions

In a turbulent flow, the presence of a wall causes a number of different effects. Near the walls, the turbulence Reynolds number approaches zero, and the mean shear normal gradients in the boundary layer flow variables become large.

At high Reynolds number the standard k-e turbulence model does not seek to directly reproduce logarithmic profiles of turbulent boundary layers, instead it applies the law of the wall in the adjacent layer (so called log-layer). The law of wall is characterized in terms of dimensionless variables with respect to boundary conditions at the wall.

The friction velocity u_τ is defined as $(\tau_w / \rho)^{1/2}$ where τ_w is the wall shear stress. Assumptions of the U as the time averaged velocity parallel to the wall and y the normal distance from the wall. The dimensionless velocity, U^+ and the dimensionless wall distance, y^+ is defined as:

$$U^+ = \frac{U}{u_\tau} \qquad \textbf{(3.12)}$$

$$y^+ = \rho \frac{u_\tau}{\mu} y \qquad \textbf{(3.13)}$$

When using this model, the value of y^+ at the first mesh point must be within the limit of validity of the wall functions, $30 < y^+ < 500$ (Versteeg and Malalasekera, 1995). The universal wall functions are valid for smooth walls. For rough walls, the

wall functions can be modified by scaling with an equivalent roughness length. However, the wall function methods are not valid in the presence of separated region or/and strong three dimensional flows. When a low Reynolds number turbulence model is used, the first node points from walls of the computational grids must be carefully allocated within the unity distance normal to the wall.

4. NUMERICAL MODEL OF THE CASE STUDY

In this chapter the experimental and the computational method will be described. In wind tunnel experiments, it is difficult to evaluate various shapes and to perform various case studies because of problems of labor and cost.

The wind tunnel model is applied in ITU as a doctoral thesis. The dimension of the model is 500*500*375 mm. It has openings on windward and leeward facades which are 410*179.4*5mm and 410*50*5 mm respectively. The aim of these openings is to produce cross ventilation inside the building as a natural ventilation method. The perspective drawing and sizes of the model is in Figure 4.1. There is a second wall on three facades except windward facades to measure the pressure difference. The distance between the two walls is 40 mm. The shading devices put on to the windward facades.

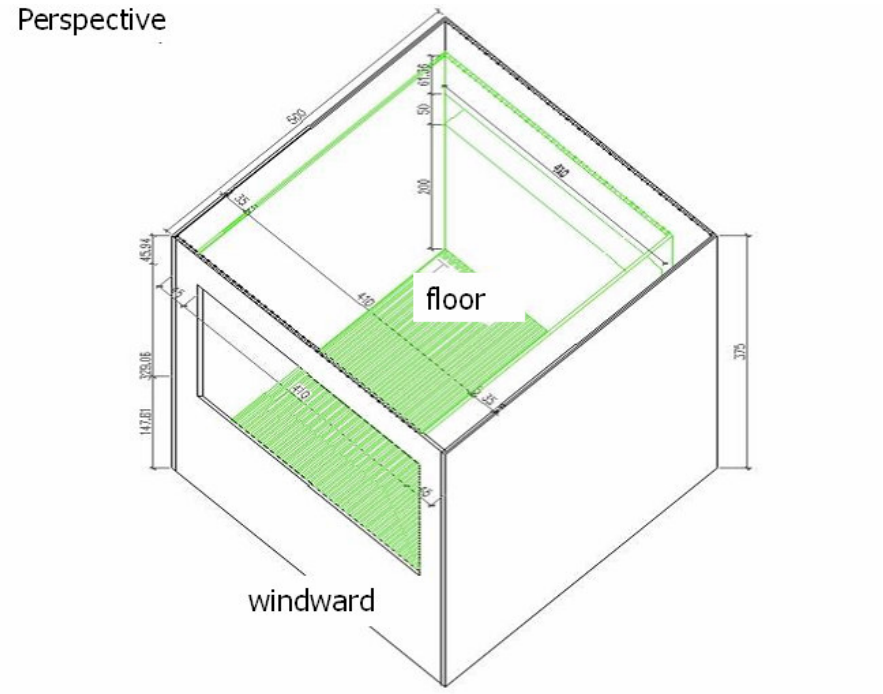

Figure 4.1 Perspective of the model (dimensions are in mm) (Ok and Turkmenoglu, 2005)

The numerical method solution is based on 2 dimensional. The size of the numerical method is shown in Figure 4.2. The 2-D of the model is considered as the middle surface on X-Y plane. The green surface is the inside wall of the leeward facades.

The dimension of the 2-D case is 500*375 mm. The opening on the windward facade is 179.4*5mm and on the leeward façade is 50*5 mm. The windward opening is 14.78 mm high from the floor; the leeward opening is 200 mm high from the floor.

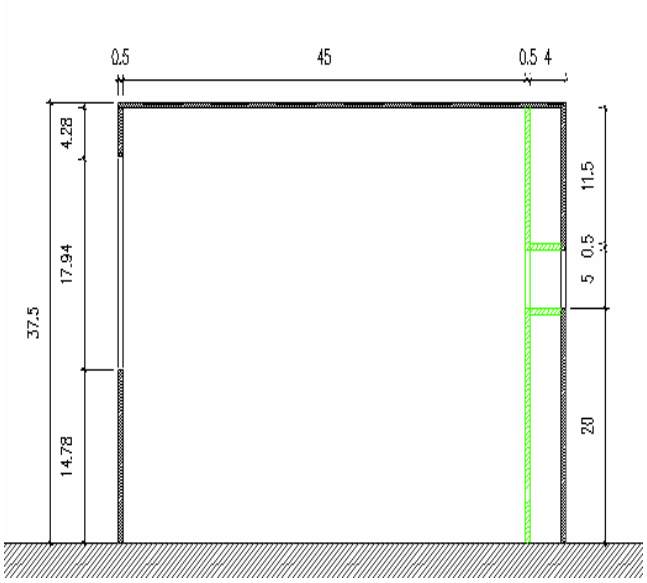

Figure 4.2: Dimensions of the 2-dimensional model (dimensions are in cm) (Ok and Turkmenoglu, 2005)

4.1 Experimental Method

In this work building surface and shading device models will be prepared by implementing some simulation techniques and rules. The effect of shading devices on interior air flows, occurring by wind pressure, will be measured in wind tunnel in constant velocity, changeable placement and with different shading device dimensions and placements

The experiments will be made in wind tunnel that is located in Istanbul Technical University Faculty of Architecture Physical Environmental Control Unit. The wind tunnel is Eiffel type and sub-sonic. The fan of the tunnel is axial fan and the power of the motor is 1.5 kW. The dimension of observation room of the wind tunnel is 1*1*3m and room is made of plexiglas and plywood. Figure 4.3 is the picture of wind tunnel in Istanbul Technical University (Ok and Turkmenoglu, 2005).

The aim of the experimental study is mostly to evaluate the effect of shading devices on solar gains. In the first step the velocity and pressure distributions is measured. The numerical method will be verified with the measured values.

Figure 4.3: The Wind Tunnel in ITU (Ok and Turkmenoglu, 2005)

4.2 Computational Model

The engineers and scientists prefer the method of Computational Fluid Dynamics because of the effectiveness, flexibility, and low labor costs. The main difficulty for the CFD is the identification of boundary conditions and parameters for the solution domain.

The computational model is solved in 2 dimensional. To get a realistic solution, the wind tunnel is included to the model in Figure 4.4. The total solution area is wind tunnel, building and various types of shading devices. The wind tunnel observation room is defined longer than the real room depending on the boundary conditions, which are defined in section 4.4. The solver for the case study is double precision and segregated. The schema of the segregated solver procedure is shown in Table 4.1. The convergency criteria for the solver are residuals<10E-6 and y^+<1 near the wall.

The dimension of the case study in computational domain is 4500*1250mm. The building is located in the centre of the x-axis.

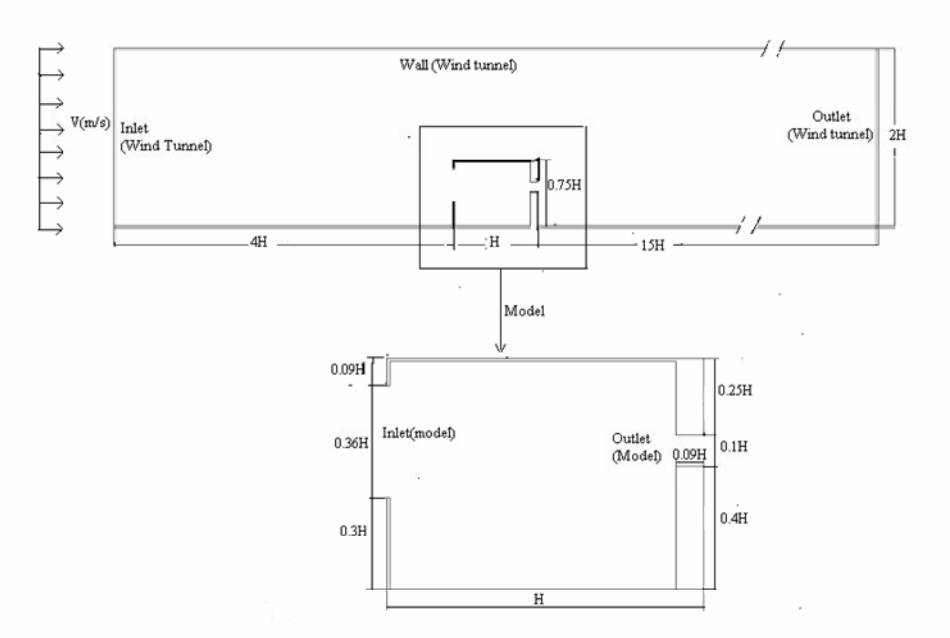

Figure 4.4: 2-D Computational Model (wind tunnel and model)

The discretization for the pressure, momentum and turbulence is made by second order discretization method. The under relaxation factors are used as defaults parameters.

Pressure: 0.2; Momentum: 0.5; Turbulence kinetic energy: 0.5;
Specific dissipation rate: 0.5

Table 4.1: Schema of the segregated solver method (Desam, 2003)

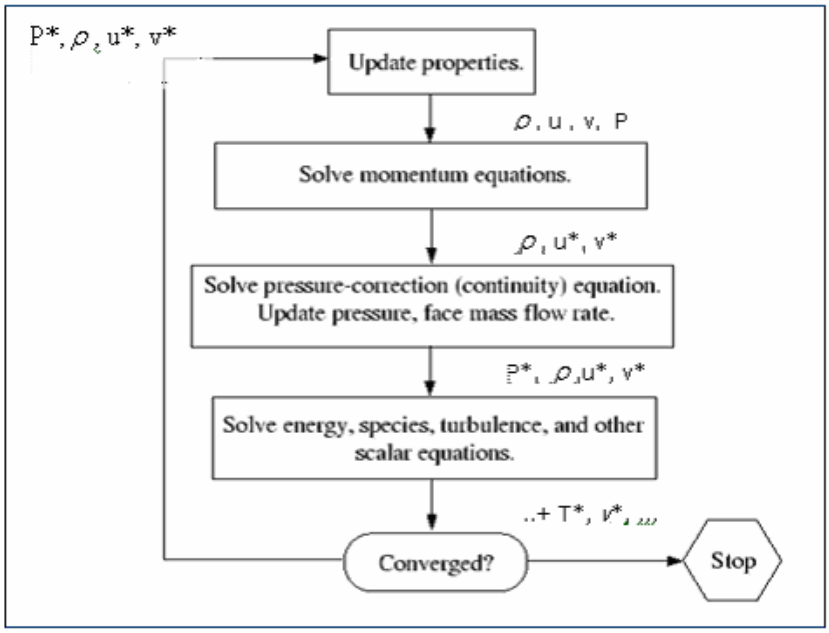

4.3 Numerical Grid

Three types of numerical grids can be used in CFD code: structured grids, unstructured grids, and combined grids.

For structured grids, algorithms can be formulated that run fast on vector computers with less computer memory required, and coarse grid generation for multigrid and the implementation of transfer operators between blocks is straightforward (Blazek, 2001).

Considering these advantages of the structured grid, the solution area divided into sub-domains which can be meshed as structured. By using these sub-domains, the solution area has more reflexibility on meshing (nonconformal mesh). These sub-domains connected each other in Fluent by the command grid interface. The consideration of these advantages the applied mesh strategy is shown in Figure 4.5. The figure represents also the unshaded case. The drawings for unshaded and shaded cases are in Appendix B.

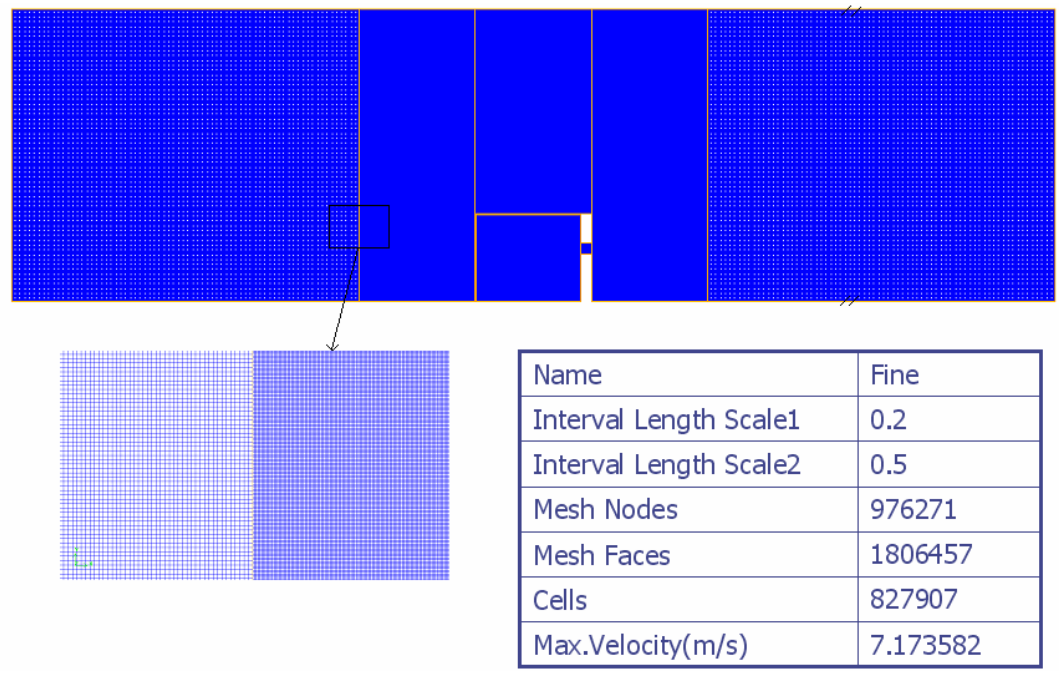

Name	Fine
Interval Length Scale1	0.2
Interval Length Scale2	0.5
Mesh Nodes	976271
Mesh Faces	1806457
Cells	827907
Max.Velocity(m/s)	7.173582

Figure 4.5 Grid of the model in Gambit

4.4 Shaded Case

The advantages of the exterior shading devices are explained in Chapter 2. Most of the researchers analyzed the effect of shading devices in the view of solar effect. Shading devices also affect the wind attributes. In this part the position of the shading device and its slat angles for the exterior shading devices are explained.

4.4.1 Horizontal Shading Devices with Parallel Slats

One of the shading devices of the solution cases is horizontal shading device case. The angle between the windward façade and the shading device is 90^0. The dimensions of the shading device are shown in Figure 4.6. The lower surface of the shading device is 331.3 mm from the floor. The total length of it is 273.1 mm, height is 43.8 mm.

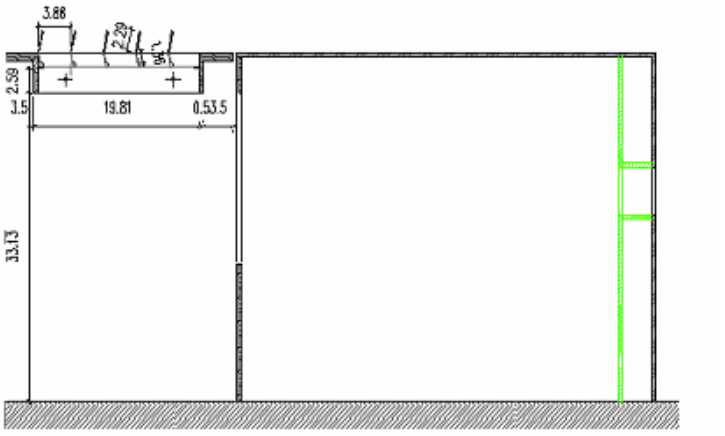

Figure 4.6: The 2-D model of model with exterior shading device (90^0 to the surface), which has 90^0 slat angle(Ok and Turkmenoglu, 2005)

The distance between the slats is 38.6 mm and it has 5 slats. The slat angles are considered as 3 types (Figure 4.7):

- 90^0 named as open-horizontal
- 45^0 named as half closed-horizontal
- 0^0 named as closed-horizontal

The detailed properties for the slat angles are defined in Section 4.4.4.

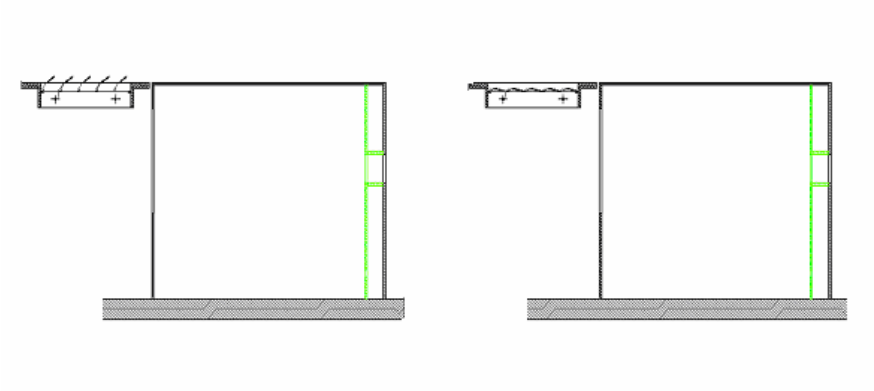

(a) (b)

Figure 4.7: The 2-D model of model with exterior shading device a) 45^0 slat angle b) 0^0 slat angle (Ok and Turkmenoglu, 2005)

4.4.2 Vertical Shading Device with Parallel Slats

Vertical shading devices are the second case for the study. The angle between the windward façade and the shading device is 0^0. The dimensions of the shading device are shown in Figure 4.8. The lower surface of the shading device is 96.9 mm from the floor. The total length of it is 273.1 mm, height is 43.8 mm.

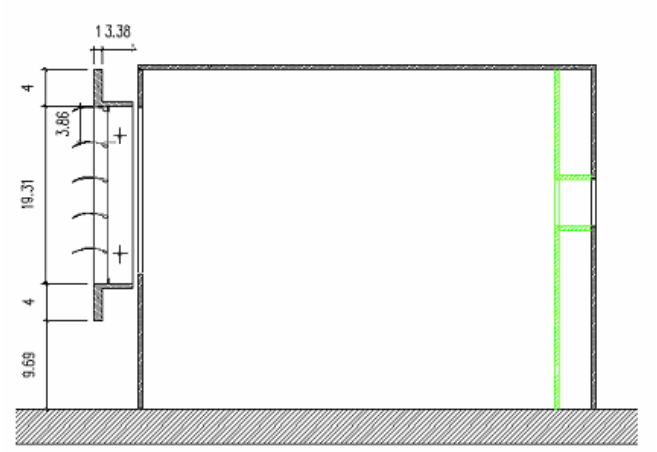

Figure 4.8: The 2-D model of model with exterior shading device (0^0 to the surface), which has 90^0 slat angle (Ok and Turkmenoglu, 2005)

The distance between the slats is 38.6 mm and it has 5 slats. The slat angles are considered as 3 types (Figure 4.9):

- 90^0 named as open-vertical
- 45^0 named as half closed-vertical
- 0^0 named as closed-vertical

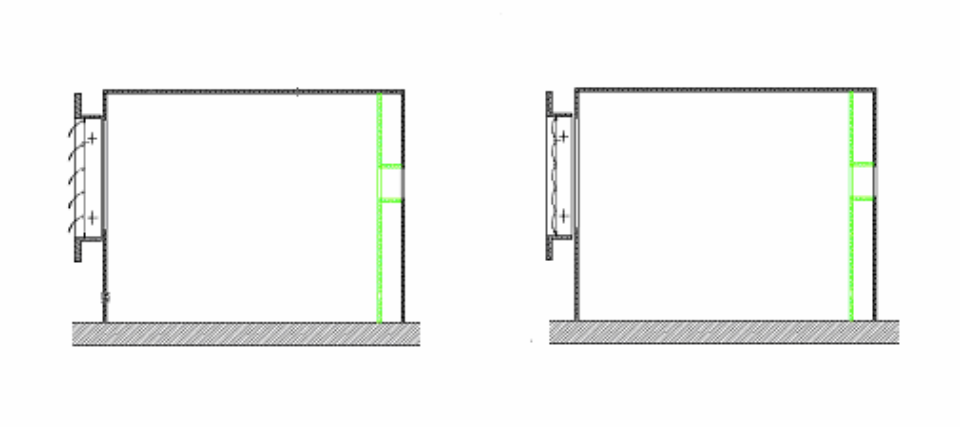

(a) **(b)**

Figure 4.9: The 2-D model of model with exterior shading device a) 45^0 slat angle b) 0^0 slat angle (Ok and Turkmenoglu, 2005)

4.4.3 Diagonal Shading Devices with Parallel Slats

Vertical shading devices are the second case for the study. The angle between the windward façade and the shading device is 45^0. The sizes of the shading device are shown in Figure 4.10. In all three cases, the dimensions of the devices are same. The lower point of the shading device is 172.8 mm from the floor.

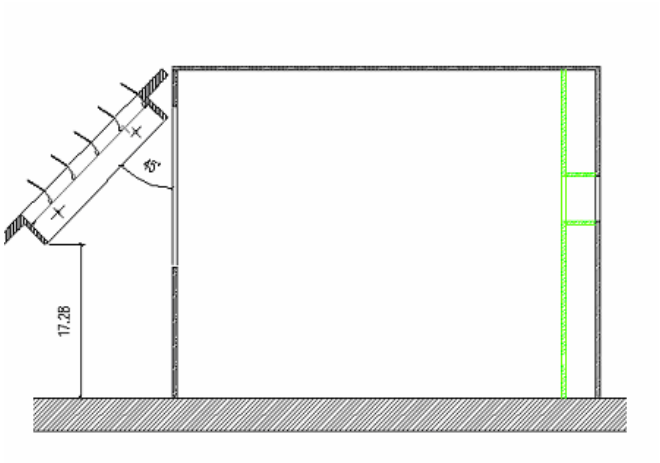

Figure 4.10: The 2-D model of model with exterior shading device (45^0 to the surface) which has 90^0 slat angle (Ok and Turkmenoglu, 2005)

The distance between the slats is 38.6 mm and it has 5 slats. The slat angles are considered as 3 types as seen in Figure 4.11:

- 90^0 named as open-diagonal
- 45^0 named as half closed-diagonal
- 0^0 named as closed-diagonal

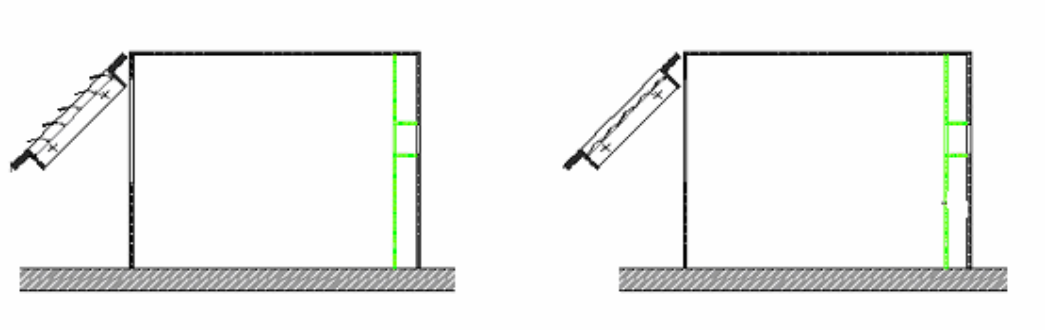

(a) **(b)**

Figure 4.11: The 2-D model of model with exterior shading device a) 45^0 slat angle b)0^0 slat angle (Ok and Turkmenoglu, 2005)

4.4.4 Slat Angles of Exterior Shading Devices

In unshaded case three position angles are defined and for each position three slat angles are defined.

- 90^0 named as closed which is shown in Figure 4.12.a. The angle of the slat is shown as 10^0
- 45^0 named as half-closed which is shown in Figure 4.12.b. The angle of the slat is shown as 35^0
- 0^0 named as open that is shown in Figure 4.12.c. The angle of the slat is shown as 80^0

The slat is also drawn in 2 dimensional in Figure .14. The slat is considered as 2 parts to mesh it as structured (normally it is spherical). The total length for the slat is 28.6 mm and the thickness is 1 mm. The number of slats is 5 and the distance between two slats is 38.6mm.

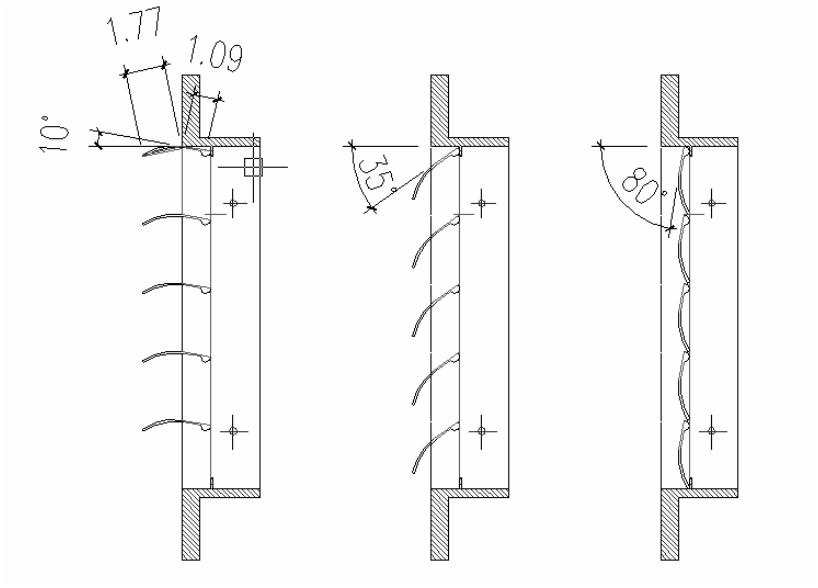

(a) (b) (c)

Figure 4.12: Slat angles of the shading devices a) 90^0 slat angle, b) 45^0 slat angle, c) 0^0 slat angle (Ok and Turkmenoglu, 2005)

4.5 Definitions and Boundary Conditions

The definitions and assumptions for the solution in Fluent Are explained in this section. Depending on this definitions and assumptions, the solution convergency is adjusted by using wall function adaptation and residuals.

4.5.1 Reynolds Number

The Reynolds number characterizes the relative importance of inertial and viscous forces in a flow. It is important in determining the state of the flow, whether it is laminar or turbulent. That means that if Re number is high, inertia forces are superior than viscosity forces and the flow is turbulent and if Re number is low, viscosity forces are superior and the flow is laminar.

Their ratio is the Reynolds number, usually denoted as Re

$$\mathrm{Re} = \frac{inertial\_force}{viscousforce} = \frac{Ud_h}{\upsilon} \qquad \textbf{(4.1)}$$

where

U velocity

d_h - hydraulic diameter

υ - kinematic viscosity

The Reynolds Number can be used to determine if flow is laminar, transient or turbulent. The flow is

- laminar if Re < 2300
- transient if 2300 < Re < 4000
- turbulent if Re > 4000

4.5.2 Hydraulic Diameter

The hydraulic diameter, d_h, is commonly used when dealing with non-circular pipes, holes or ducts.

The definition of the hydraulic diameter is:

$$\mathrm{Re} \equiv 4\frac{cross-\sec tional-area-of-duct}{wetted-perimeter-of-duct} \quad \textbf{(4.2)}$$

Using the definition above the hydraulic diameter can easily be computed for any type of duct-geometry. Below follows a few examples.

4.5.3 Turbulence Intensity

When setting boundary conditions for a CFD simulation it is often necessary to estimate the turbulence intensity on the inlets.

The turbulence intensity is defined as:

$$I = \frac{u'}{U} \quad \textbf{(4.3)}$$

Where u`is the root-mean-square of the turbulent velocity fluctuations and U is the mean velocity (Reynolds averaged).

If the turbulent energy, k, is known u' can be computed as:

$$u' = \sqrt{\frac{2}{3}k} \quad \textbf{(4.4)}$$

For fully developed pipe flow the turbulence intensity at the core can be estimated as:

$$I = 0.16\,\mathrm{Re}_{dh}^{-\frac{1}{8}} \quad \textbf{(4.5)}$$

Where Re_{dh} is the Reynolds number based on the pipe hydraulic diameter d_h.

4.5.4 Wall functions (y+)

A non-dimensional wall distance for a wall-bounded flow can be defined in the following way:

$$y^+ \equiv \frac{u_* y}{\upsilon} \quad \textbf{(4.6)}$$

y^+ is used in boundary layer theory and in defining the law of the wall. The computational problem is solved till the $y^+<1$ as one of the convergence criteria.

4.5.5 Pressure Coefficient

The pressure coefficient is a dimensionless number used in aerodynamics and fluid mechanics, most often in the design and analysis of an airfoil. The relationship between the coefficient and the dimensional number is:

$$C_p = \frac{p - p_\infty}{\frac{1}{2}\rho V^2} \quad \textbf{(4.7)}$$

where

p is the static pressure

p_∞ is the free stream pressure

ρ is the fluid density (sea level air is 1.225kg/m3)

C_p of zero indicates the pressure is the same as the free stream pressure

4.5.6 Definitions and Boundary Conditions

4.5.6.1 Inlet Boundary Conditions

The Inlet velocity is 2.5 m/s uniform velocity. However, to get a realistic solution in Computational domain, the flow should be fully developed and there should be boundary layer. Because of that, the inlet boundary is four times far away from the real condition.

4.5.6.2 Outlet Boundary Conditions

The outlet boundary condition defined as pressure outlet, which means the deviation of the pressure depending on the length is zero. To get this condition, the outlet of the computational domain is assumed 15 times far away from the real condition.

4.5.6.3 Wall Boundary Conditions

In this research, it is solved only airflow phenomena. Because of that, all the other surfaces (except inlet and outlet) are assumed as wall boundary condition.

The definitions and boundary conditions for the model is summarized in Table 4.2.

Table 4.2: The Solver and boundary conditions

Platform		FLUENT 6.2
Algorithm		SIMPLEC
Differencing Scheme	u, v, w (velocity)	Second Order
	k, e (RNG)	Turbulence intensity (0.04) and hydraulic diameter(2.1)
Boundary Conditions	Inlet	Velocity profile is uniform(2.5 m/s)
	Outlet	The gradient of pressure is taken to be zero
	Wall	Enhanced wall functions
Turbulence Intensity		%4
Wind direction		Normal to the surface

5. RESULTS OF THE CASE STUDY

5.1 Grid Independency

As a validation parameter of the solution method grid independency is checked for unshaded cases and the same results assumed for the shaded cases. The parameter of the independency is the pressure coefficient on the upper wall of the room in solution domain. Different grid length scales applied to the domain and the less pressure coefficient distribution between two grids is accepted. The grid sizes and calculated maximum velocity in the computational domain are summarized in Table 5.1.

Table 5.1: Grid sensitivity

Mesh properties for the model without shading devices			
Name	Fine	Medium	Coarse
Interval Length Scale1	0.5	1	2
Interval Length Scale2	1	2	4
Mesh Nodes	429171	350561	340581
Mesh Faces	768616	617796	597035
Cells	338599	266727	256142
Max.Velocity(m/s)	4.628272	4.895605	4.757018

Table 5.2 shows the mass flow rate of the inlet, outlet, and net for each model. The mass flow rate of inlet and outlet should be equal to each other; there is no external mass flow rate. The net Flow rate gives an idea for the iteration errors.

Table 5.2: Mass Flow Rate

Boundaries	Fine	Medium	Coarse
Inlet	3.8281251	3.8281251	3.8281251
Outlet	-3.8281148	-3.8294139	-3.828294
Net	10.29761e-06	- 1288.748e-06	- 168.89344e-06

The main aim of the grid analysis is to satisfy the grid independency on the computational calculations. The basic parameter for independency is pressure coefficient, Cp, which is defined in Chapter 4. As seen in Figure 5.1, Cp values vary depending on the grid size. When the length scale of the grid is high, the variation of Cp value is high.

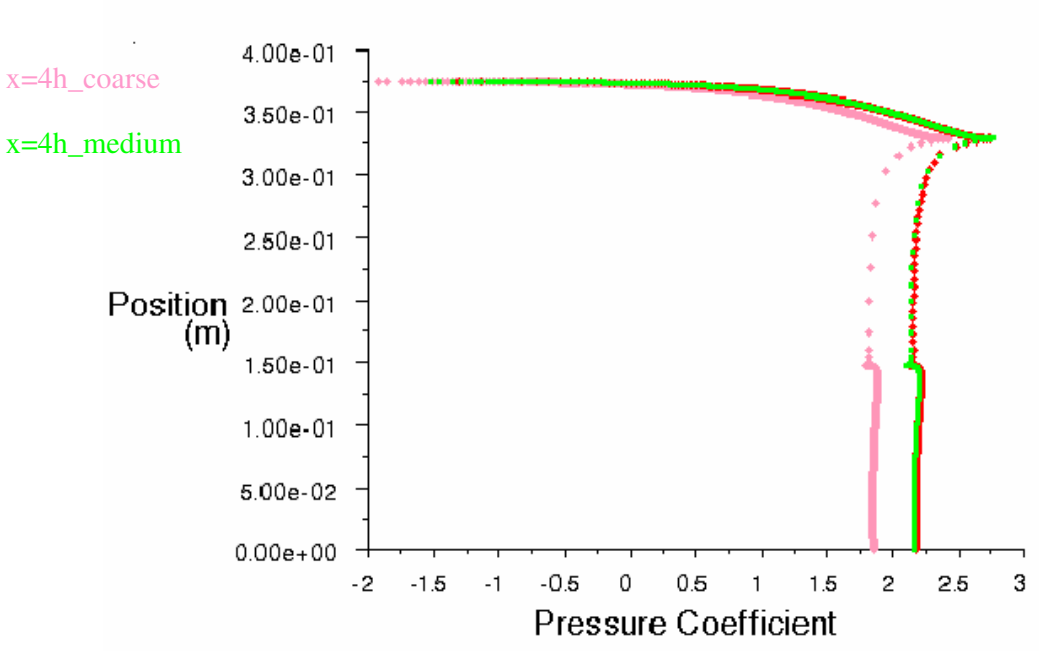

Figure 5.1: Pressure coefficient profiles for grid sensitivity on windward

Coarse, medium, and fine length scale models' pressure coefficients variations are compared and fine length scale model for unshaded case is obtained as a reference point for other cases.

5.2 Results for all the Cases

In this part, the distributions for velocity, pressure coefficient and pathlines around and inside the room are defined for each case study that explained in Section 4.

5.2.1 Unshaded Case:

5.2.1.1 Velocity Profile for Unshaded Case

In this case, the model has openings on windward and leeward walls. The separation occurs on the top point of windward wall. The velocity gets the highest value, app.7 m/s. The shear layer increases and the pressure decrease in this wake. At the bottom of the windward wall, the velocity is app. 0m/s, because the flow is fully developed and the bottom region has shear layer. At this part, there occurs vorticity.

As a key point of the solutions, velocity profile is shown in Fig 5.2 at the center of the room which is x= 4.5h, x=0.75h (0.375m) is the upper surface of the room. The maximum velocity inside the room is 1.8m/s where is on the upper side of the room.

The maximum velocity outside of the room is 5.2 m/s on the exterior of room upper wall.

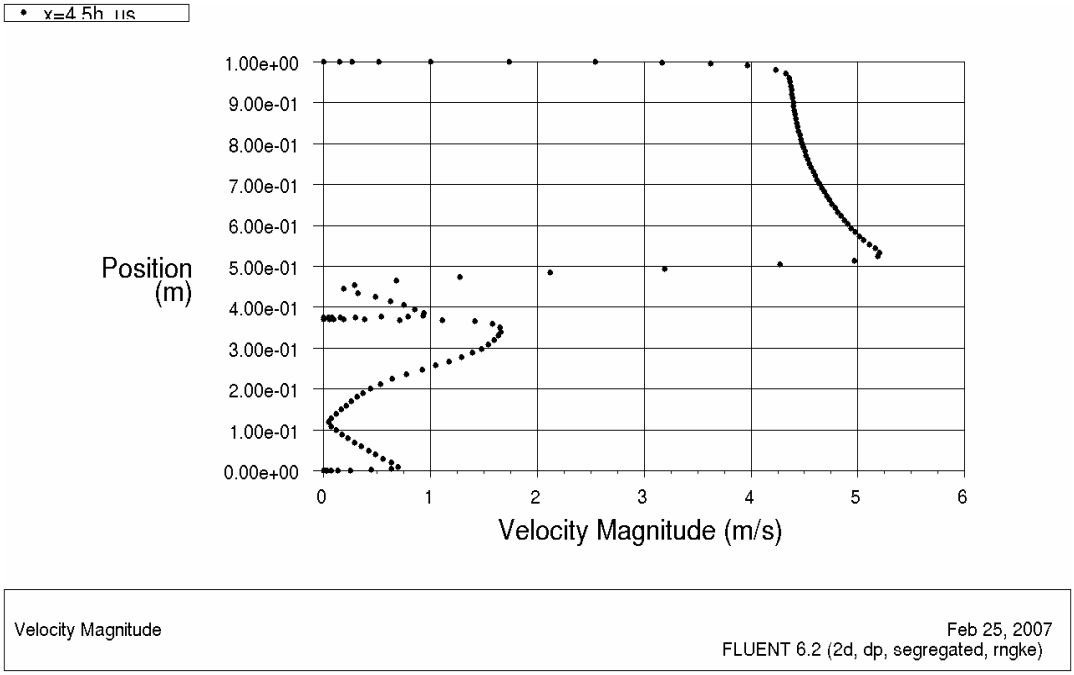

Figure 5.2: Velocity profile at x=4.5h for unshaded devices

5.2.1.2 Pressure Coefficients for Unshaded Case

Pressure coefficients of the room three walls (windward, upperwall, and leeward) are observed as seen in Fig. 5.3, Fig. 5.4 and Fig.5.5 in respectively. On windward, pressure coefficient reaches at a value +2.3 where is closed to the openings upside. The minimum pressure coefficient is app. –1.5 where is the separations' starting point.

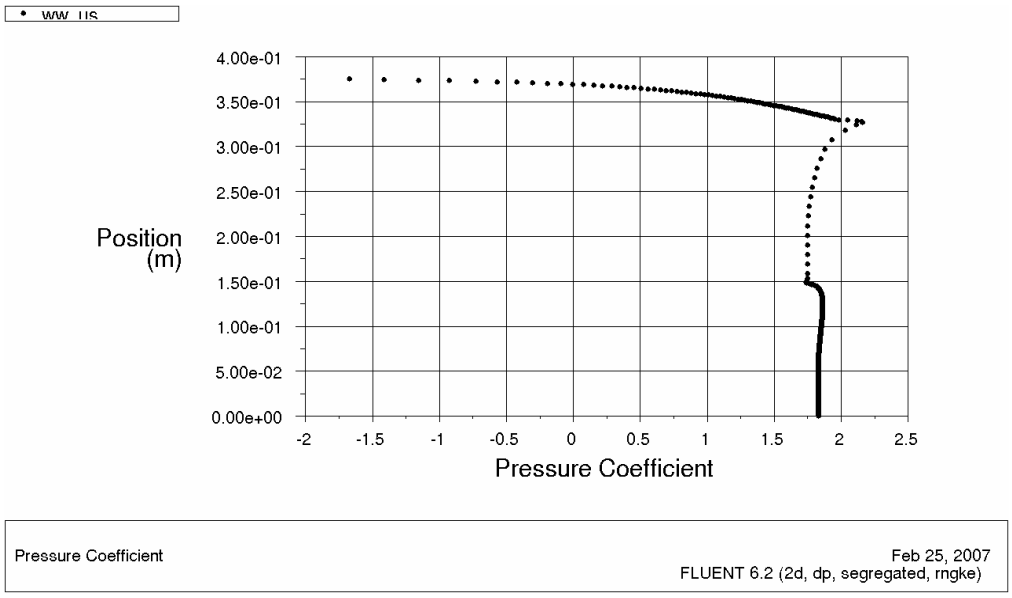

Figure 5.3: Pressure coefficient profiles for unshaded case on windward

On the upper wall, pressure coefficient reaches maximum –2.27 and min.-2.6. The shape of the pressure coefficient diagram on upper wall shows the pressure distribution and gives an idea about the shape of the bubbles on the outside exterior of the upper wall.

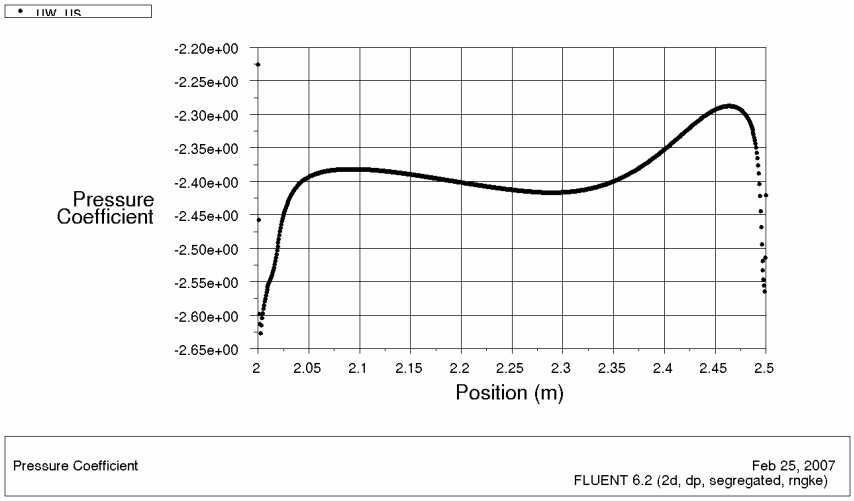

Figure 5.4: Pressure coefficient profiles for unshaded case on upper wall

On leeward, pressure coefficient reaches at a value –1.3 where is closed to downside wall of the room. The minimum pressure coefficient is app. –2.2 where is closed to upside of the leeward.

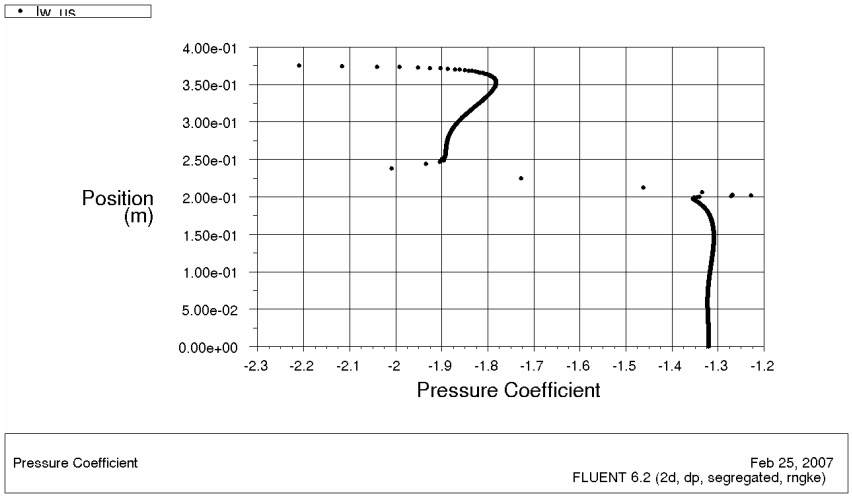

Figure 5.5: Pressure coefficient profiles for unshaded case on leeward

5.2.1.3 Pathlines for Unshaded Case

Unshaded case is solved and figured as a baseline for other cases. In this part the pathlines are drawn for unshaded case and figured in Figure 5.6 a and b which show the airflow on whole solution area and around and inside the room respectively. There is three main wakes on solution area where upper, inner and back sides of the room. When the solution area is analyzed in detailed as seen in Fig. 5-6-b, in front of the room there is a wake also depending on the boundary layer effect. On the lower side of the leeward there occurs a death zone as the same reason of front side.

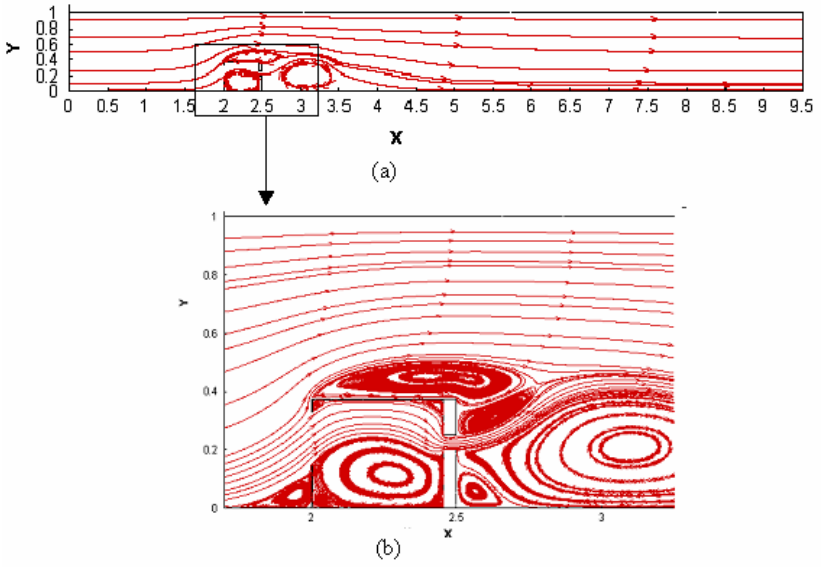

Figure 5.6: Velocity pathlines for the unshaded case a) total area b) detailed (close to model)

5.2.2 Horizontal Shading Devices

Horizontal shading devices has three cases; open, half open, and closed as explained in model definition part.

5.2.2.1 Velocity Profiles for Horizontal Shading Devices

The velocity magnitude increases depending on the slat angles. When the case is closed which means the angle of slat angle is 0, the maximum velocity is 10m/s. In open-horizontal case (slat angle is 90), velocity magnitude reaches 4.5m/s. Maximum velocity for the half-closed horizontal case (slat angle 45) is 6.5 m/s. The velocity profiles of this cases summarized in Figure 5.7 at x=4.5 h where is the center of the room in x-axis..

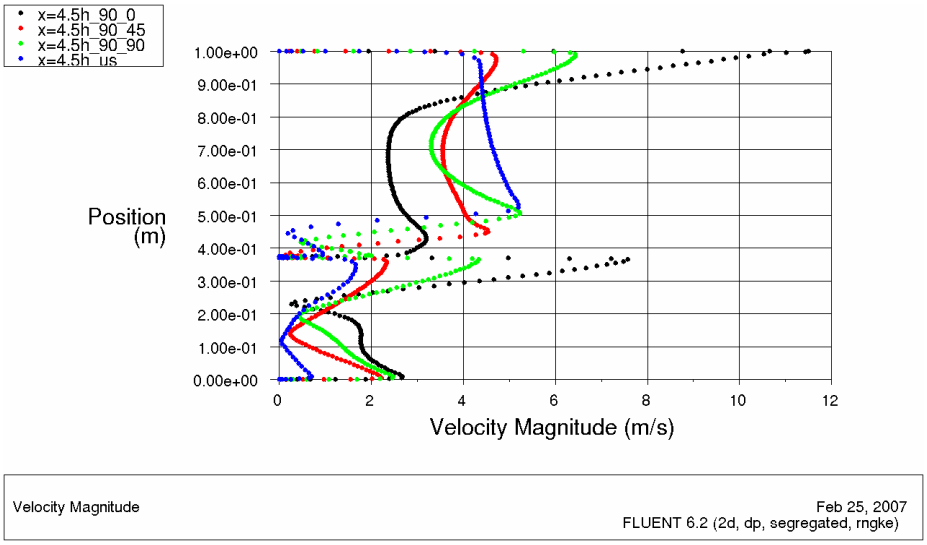

Figure 5.7: Velocity profiles for horizontal shading devices (90_0, 90_45, 90_90) and unshaded at x=4.5h

In these cases, the model has openings on windward and leeward walls and in front of the windward, there is located a shading devices with an angle 90 to the windward face. The separation occurs on the top point of windward wall for all horizontal cases.

5.2.2.2 Pressure Coefficient for Horizontal Shading Devices

Pressure coefficients of the windward for horizontal cases are drawn in Fig. 5.8. On windward, pressure coefficient for closed case reaches at a value +27 where is closed to the down of the windward. The minimum pressure coefficient is app. +9.5 where

is closed to the upper wall intersection. On windward, pressure coefficient for half_closed case reaches at a value +5 where is closed to the down of the windward. The minimum pressure coefficient is app. –2 where is closed to the upper wall intersection. Pressure coefficient for open case reaches at a value +4 where is closed to the down of the windward. The minimum pressure coefficient is app. -3 where is closed to the upper wall intersection.

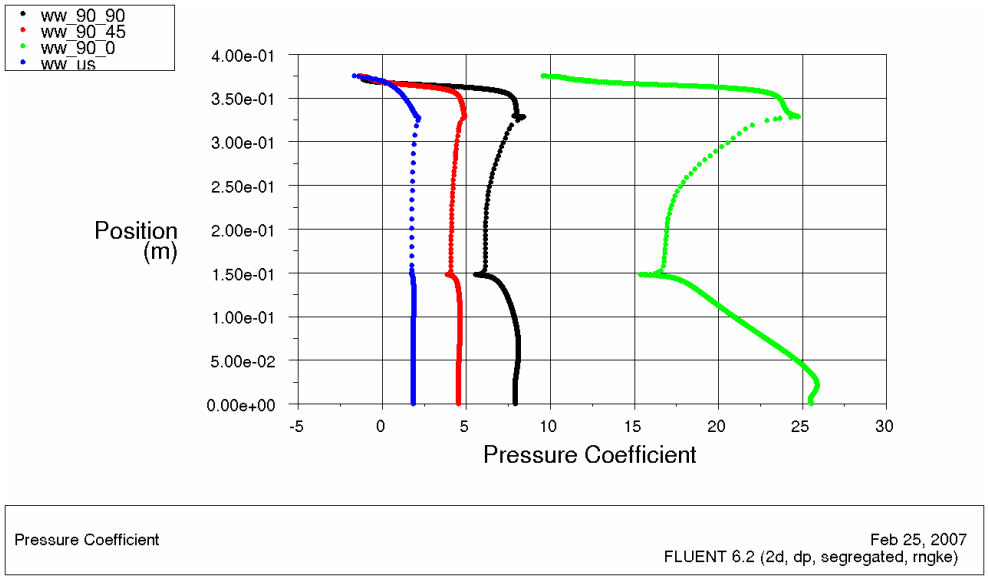

Figure 5.8: Pressure coefficient profiles for horizontal shading devices (90_0, 90_45, 90_90) and unshaded on windward

On the upper wall that is shown in Fig.5.9, pressure coefficient for closed case reaches maximum +12 and min. +9. On the upper wall, pressure coefficient for half_closed case reaches at a value +0.5where is closed to the down of the windward. The minimum pressure coefficient is app. –1 where is closed to the upper wall intersection. The pressure coefficient for open case max value is +1.95 and min is –1.5. The shape of the pressure coefficient diagram on upper wall shows the pressure distribution and gives an idea about the shape of the bubbles on the outside exterior of the upper wall.

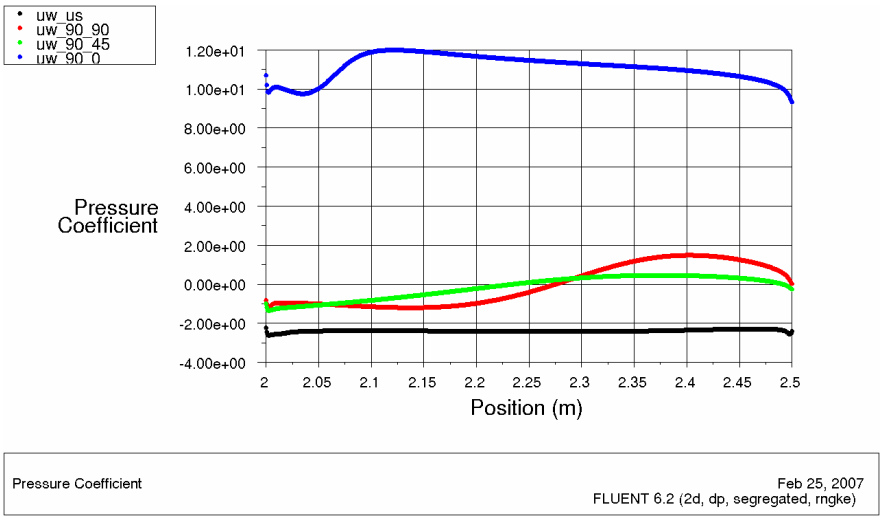

Figure 5.9: Pressure coefficient profiles for horizontal shading devices (90_0, 90_45, 90_90) and unshaded on upper wall

On leeward that is shown in Fig.5.10, pressure coefficient for closed case reaches maximum +11 and min. +7.5. On the upper wall, pressure coefficient for half-closed case reaches at a value +1 where is closed to the down of the windward. The minimum pressure coefficient is app. –1 where is closed to the upper wall intersection. The pressure coefficient for open case max value is –1.2 and min is –2.2.

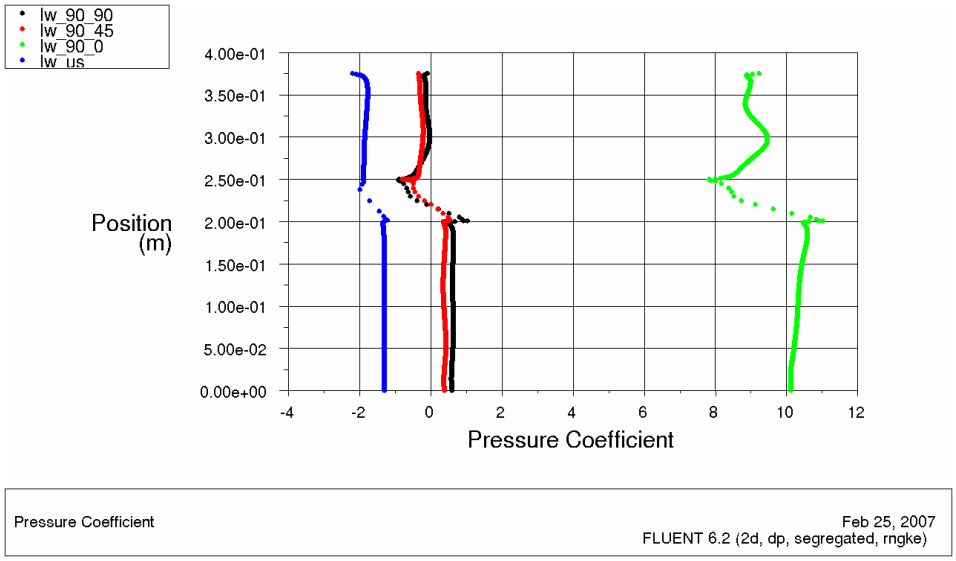

Figure 5.10: Pressure coefficient profiles for horizontal shading devices (90_0, 90_45, 90_90) and unshaded on leeward

5.2.2.3 Pathlines for Horizontal Shading Devices

The pathlines for horizontal cases are analyzed in this part and drawn in Figures 5.11- 5.14. Each figure shows separate horizontal cases airflow on the solution area and around and inside the room.

In open horizontal case, slats directed the airflow to the upper side of the solution dommain. When looking at the solution as general in Fig 5.11, there is three main vortexes on solution domain where are upper, inner and back sides of the room. Comparisons with the unshaded case the shape of these vortexes are changed. By the forcing effect of open slats on airflow the upper side vortex is getting wider but shorter. Inside vortex covers all the room. At the back side of the room the wake is getting narrower (the height of the wake is shorter). Front wall wake which occurs depending on the boundary layer is minimized.

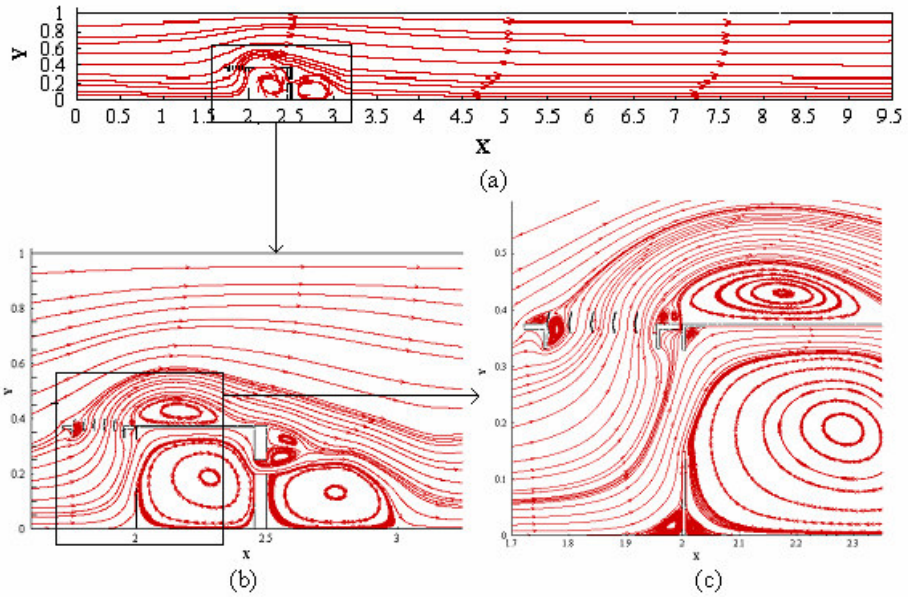

Figure 5.11: Velocity pathlines for open-horizontal shading devices (90_90) a) total area b) area between x=1.7-3.25 c) area between x 1.7-2.35

In half closed horizontal case, slats directed the airflow to the upper side of the solution domain smoothly. When looking at the solution as general in Fig 5.12, there is two main vortexes on solution domain where are inner and back sides of the room. Comparing with the unshaded case the shape of these vortexes are changed. By the forcing effect of half_closed slats on airflow the upper side vortex is almost lost. The slats minimized the bubble on the upper wall. Inside, vortex covers all the room. At

the back side of the room the wake is getting narrower (the height of the wake is shorter). Front wall wake, which occurs depending on the boundary layer, is minimized.

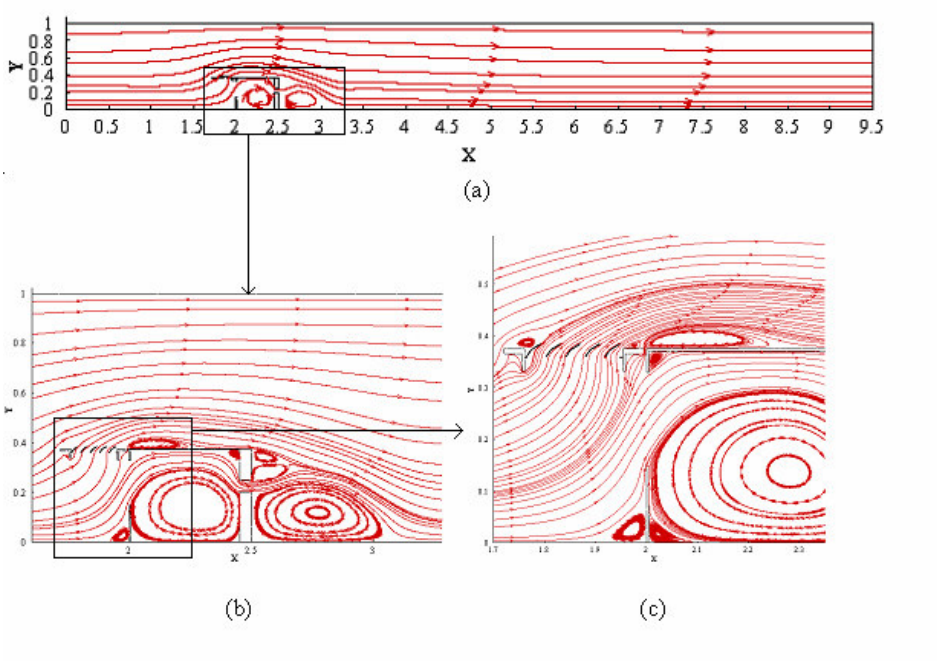

Figure 5.12: Velocity pathlines for halfopen-horizontal shading devices (90_45) a) total area b) area between x=1.7-3.25 c) area between x 1.7-2.35

In closed horizontal case, slats are totally closed and this condition is raised like a second cavity problem. Inside and frontal area of the room have cavity like flow mechanism. The closed horizontal shading device behaves like a wall. As a result of this condition, (mentioned above) the whole airflow forced to the room and the pressure coefficient is increased. Depending on the leakage between the shading device and room, on the upper side of the wall has two bubbles, one is on the shading device and the other is on the upper wall. The upper wall bubble is relatively smaller than the shading device bubble which are shown in Fig5.13. Inside, vortex covers all the room. At the back side of the room the wake is getting narrower comparing with the unshaded case (the height of the wake is shorter). Front wall wake, which occurs depending on the boundary layer, is minimized.

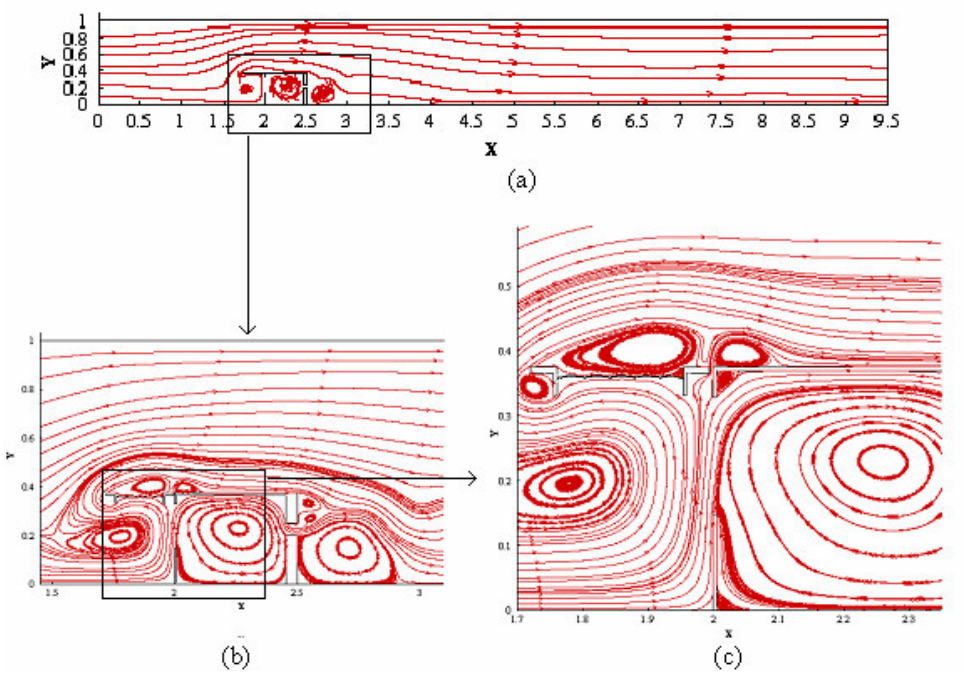

Figure 5.13: Velocity pathlines for closed-horizontal shading devices (90_0) a) total area b) area between x=1.7-3.25 c) area between x 1.7-2.35

Figure 5.14 is a short review of horizontal cases. It is easy to compare open, half-closed and closed cases. The shapes of bubbles around and inside the room are seen obviously. Especially the closed case has significant difference. The flow inside and front of the room behaves like a cavity flow and the vortex on the upper wall has two wakes. The smoothest airflow behavior around and inside the room occurs in the half closed case due to the slat angle's airflow forcement.

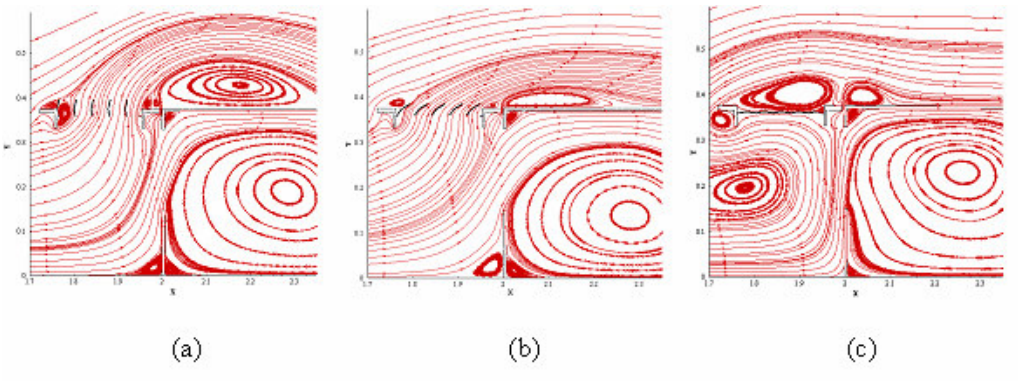

Figure 5.14: Pathlines comparison between slats of a) 90_0, b) 90_45, c) 90_90

5.2.3 Vertical Shading Devices

Vertical shading devices has three cases; open, half open, and closed as explained in model definition part.

5.2.3.1 Velocity Profiles for Vertical Shading Devices

The velocity magnitude increases depending on the slat angles. When the case is closed which means the angle of slat angle is 0, the maximum velocity is 5.5m/s. In open-vertical case (slat angle is 90), velocity magnitude reaches 4.2m/s. Maximum velocity for the half-closed vertical case (slat angle 45) is 6.5 m/s. The velocity profiles of this cases summarized in Figure 5.15.

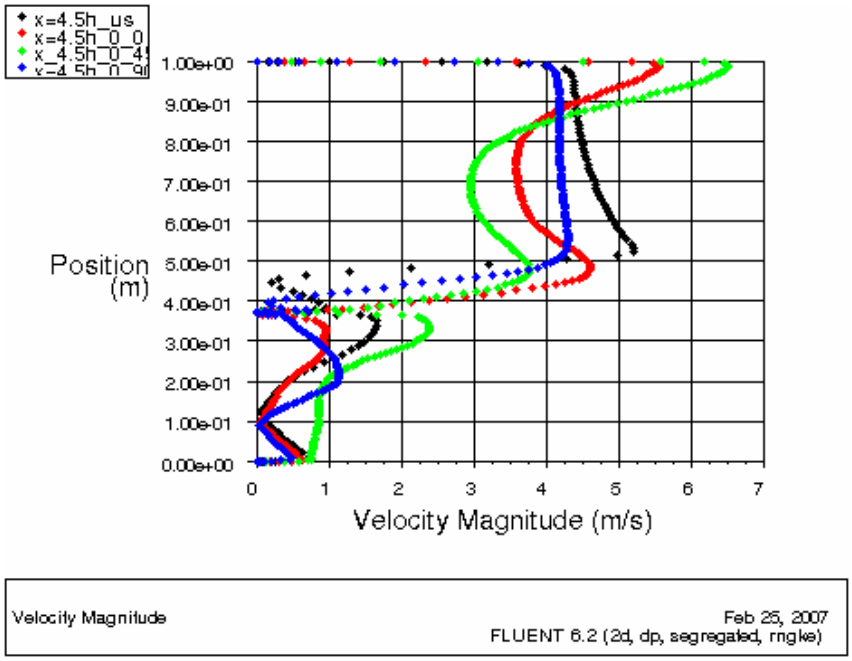

Figure 5.15: Velocity profiles for vertical shading devices and unshaded case at x=4.5h

5.2.3.2 Pressure Coefficient for Vertical Shading Devices

Pressure coefficients of the windward for vertical cases are drawn in Fig. 5.16. On windward, pressure coefficient for closed case reaches at a value +5.8 where is closed to the down of the windward. The minimum pressure coefficient is app. -3 where is closed to the upper wall intersection. On windward, pressure coefficient for half_closed case reaches at a value +7 where is closed to the down of the windward. The minimum pressure coefficient is app. –1.5 where is closed to the upper wall

intersection. Pressure coefficient for open case reaches at a value +3 where is closed to the down of the windward. The minimum pressure coefficient is app. -3 where is closed to the upper wall intersection.

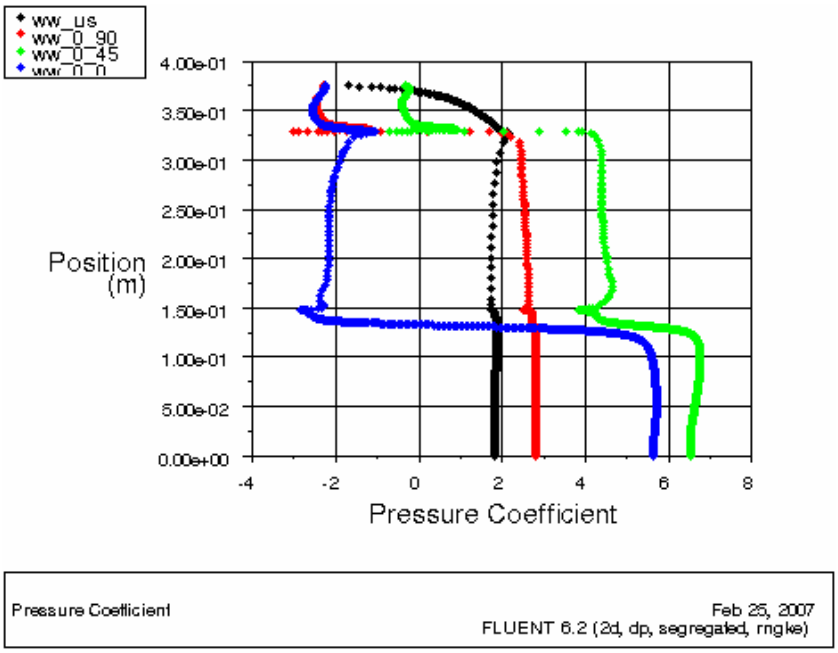

Figure 5.16: Pressure Coefficient profiles for horizontal shading devices (0_90, 0_45, 0_0) and unshaded case on windward

On the upperwall that is shown in Fig.5.17, pressure coefficient for closed case reaches maximum +0.7and min.-2.4. On the upperwall, pressure coefficient for half_closed case reaches at a value +1.5where is closed to the down of the windward. The minimum pressure coefficient is app. –0.25 where is closed to the upper wall intersection. The pressure coefficient for open case max value is –0.5 and min is –2.25. The shape of the pressure coefficient diagram on upper wall shows the pressure distribution and gives an idea about the shape of the bubbles on the outside exterior of the upper wall.

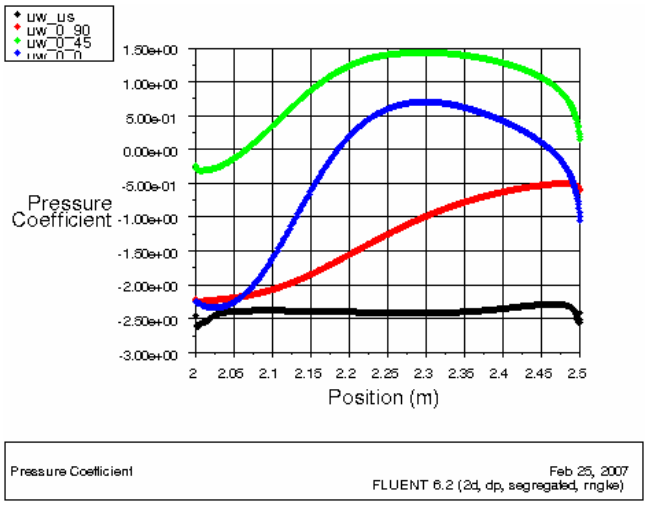

Figure 5.17: Pressure Coefficient profiles for horizontal shading devices (0_90, 0_45, 0_0) and unshaded case on upper wall

On leeward that is shown in Fig.5.18, pressure coefficient for closed case reaches maximum –0.2 and min.-3.5. On the upperwall, pressure coefficient for half-closed case reaches at a value +1.8 where is closed to the down of the windward. The minimum pressure coefficient is app. –0.1 where is closed to the upper wall intersection. The pressure coefficient for open case max value is –0.2 and min is –0.8.

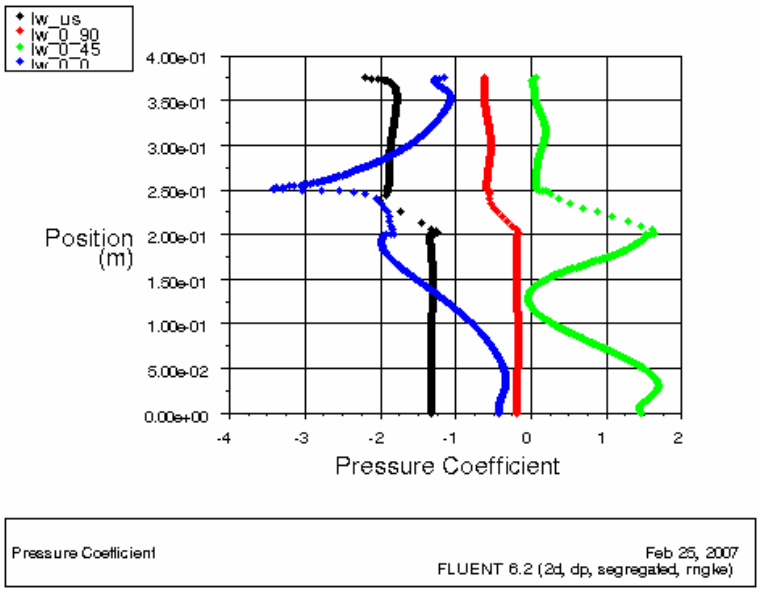

Figure 5.18: Pressure Coefficient profiles for horizontal shading devices (0_90, 0_45, 0_0) and unshaded case on leeward

5.2.3.3 Path lines for Vertical Shading Devices

The pathlines for vertical cases are analyzed in this part and drawn in Figures 5.18-5.21. Each figure shows separate vertical cases, which are open, half-closed, and closed cases, airflow on the solution domain and around and inside the room.

In open vertical case, slats directed the airflow to room. When looking at the solution as general in Figure 5.19 there is three main vortexes on solution domain where upper, inner and back sides of the room. Comparing the unshaded case and the open vertical case, the shape of these vortexes are not changed unlike horizontal cases The open slats directed the flow smoothly to the room and the airflow behaves like unshaded case inside the room. The vortex is narrower and the bubble in front of the front of the front wall, which occurs depending on the shear forces on the floor, is bigger than the horizontal cases.

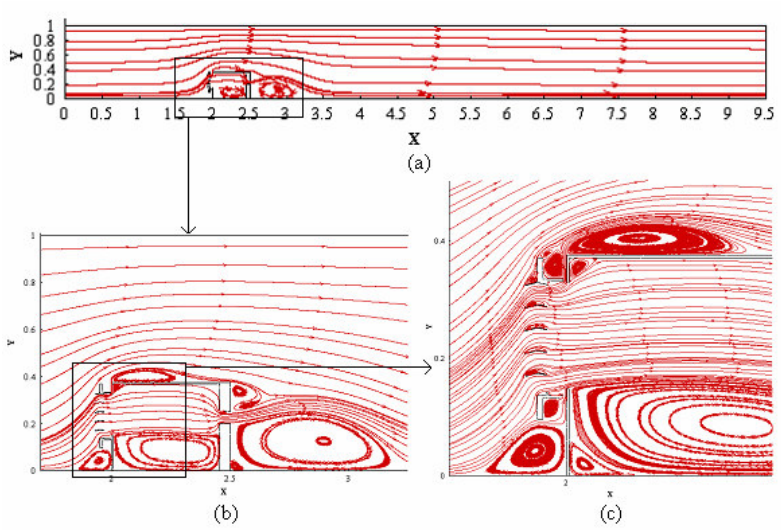

Figure 5.19: Pathlines for open-vertical shading devices (0_90) and unshaded case
a) total area b) x=1.7-3.25 c) x= 1.8-2.35

In half closed vertical case, slats directed the airflow to the upper side of the room. When looking at the solution domain as general in Fig 5.20, there is two main vortexes on solution area where inner and back sides of the room. Due to the movement of the airflow, the vortex inside the room covers almost all the room. The bubble ,which normally seems on the upside of the upper wall, is getting minimum comparing with the vertical cases. The wind ward and leeward's vortexes are also minimized.

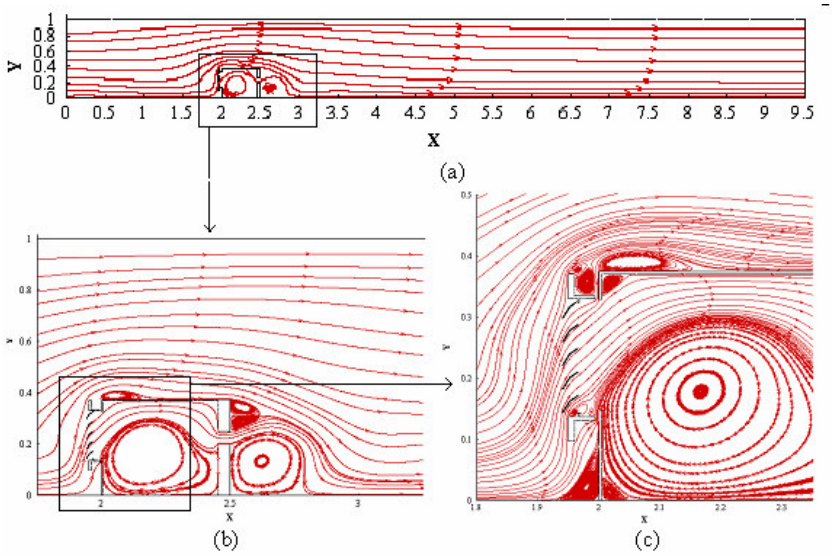

Figure 5.20: Pathlines for halfopen-vertical shading devices (0_45) and unshaded case a) total area b) x=1.7-3.25 c) x= 1.8-2.35

Figure 5.21 shows the closed vertical case solution domain as general and detailed. When looking at the general view, there seems three bubbles, where are inside and backside of the room. The maiin difference from the other two vertical cases is the location of the bubbles. Two of the three vertical cases occurs inside of the room which are main vortex behavior and relatively small vortexes. The shape of the room inside vortexes are caused by the leakage between the shading device and the room. The shear layer vortex in front of the room is almost disappeared.

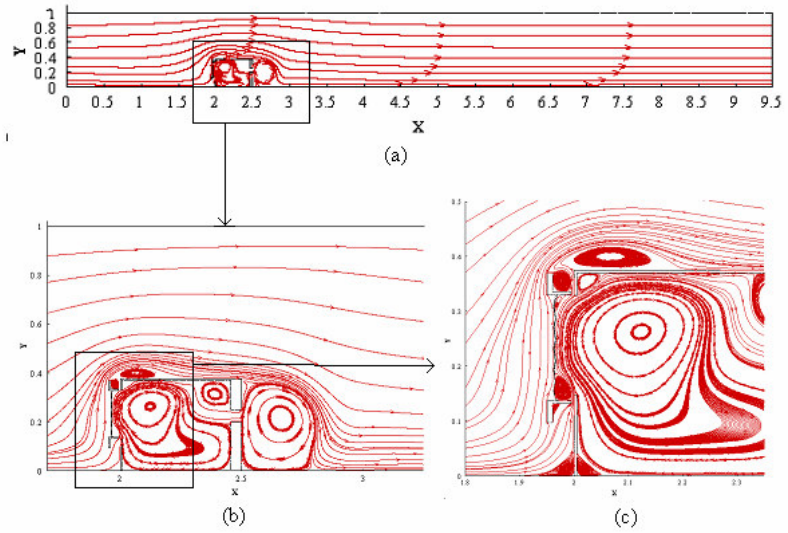

Figure 5.21: Pathlines for closed vertical shading devices (0_0) and unshaded case a) total area b) x=1.7-3.25 c) x= 1.8-2.35

Figure 5.22 is a short review of three vetical cases which gives an idea of the effects of slats angle on vertical shading devices' airflow. The shapes of the bubbles around and inside the room are seen obviously. At the room inside flow behavior point, the best case seems open vertical case. However, this condition causes a maximizing on the windward and upperwall vortexes'.

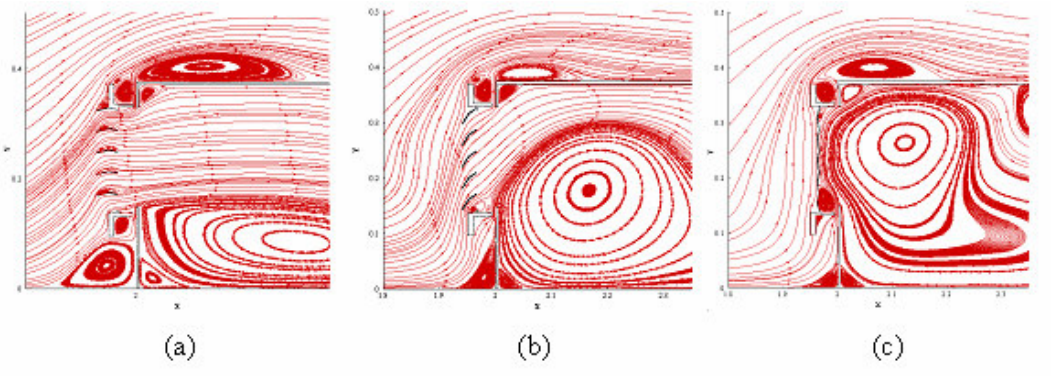

Figure 5.22: Pathline comparison between three vertical cases a) 0_90 b) 0_45 c) 0_0

5.2.4 Diagonal Shading Devices

Diagonal shading devices has three cases; open, half open and closed as explained in model definition part.

5.2.4.1 Velocity Profiles for Diagonal Shading Devices

The velocity magnitude increases depending on the slat angles. When the case is closed which means the angle of slat angle is 0, the maximum velocity is 5.2m/s. In open-diagonal case (slat angle is 90), velocity magnitude reaches 6.5 m/s. Maximum velocity for the half-closed diagonal case (slat angle 45) is 4.6 m/s. The velocity profiles of this cases summarized in Figure 5.23.

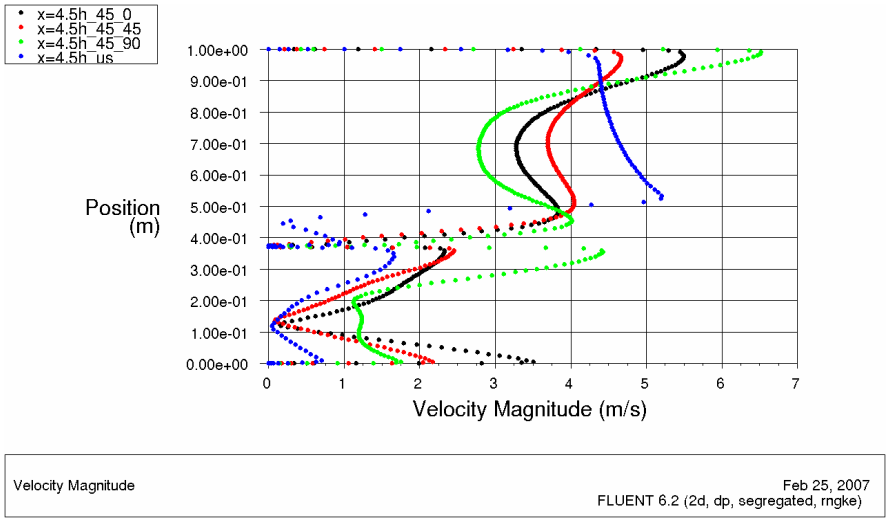

Figure 5.23: Velocity profiles for diagonal shading devices (45_90, 45_45, 45_0) and unshaded case at x=4.5h

5.2.4.2 Pressure Coefficients for Diagonal Shading Devices

Pressure coefficients of the windward for vertical cases are drawn in Fig. 5.24. On windward, pressure coefficient for closed case reaches at a value +2 where is closed to the down of the windward. The minimum pressure coefficient is app. -2 where is closed to the upper wall intersection. On windward, pressure coefficient for half_closed case reaches at a value +8.5 where is closed to the down of the windward. The minimum pressure coefficient is app. –0.5 where is closed to the upper wall intersection. Pressure coefficient for open case reaches at a value +4.2 where is closed to the down of the windward. The minimum pressure coefficient is app. –1.6 where is closed to the upper wall intersection

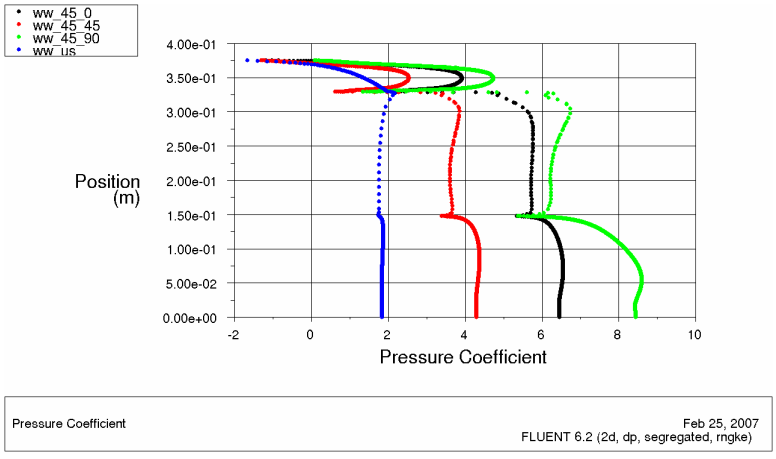

Figure 5.24: Pressure Coefficient profiles for diagonal shading devices (45_90, 45_45, 45_0) and unshaded case on windward

On the upperwall that is shown in Fig.5.25, pressure coefficient for closed case reaches maximum –2.2 and min.-2.6. On the upperwall, pressure coefficient for half_closed case reaches at a value +0.5where is closed to the down of the windward. The minimum pressure coefficient is app. –1.2 where is closed to the upper wall intersection. The pressure coefficient for open case max value is 1.4 and min is –1.3. The shape of the pressure coefficient diagram on upper wall shows the pressure distribution and gives an idea about the shape of the bubbles on the outside exterior of the upper wall.

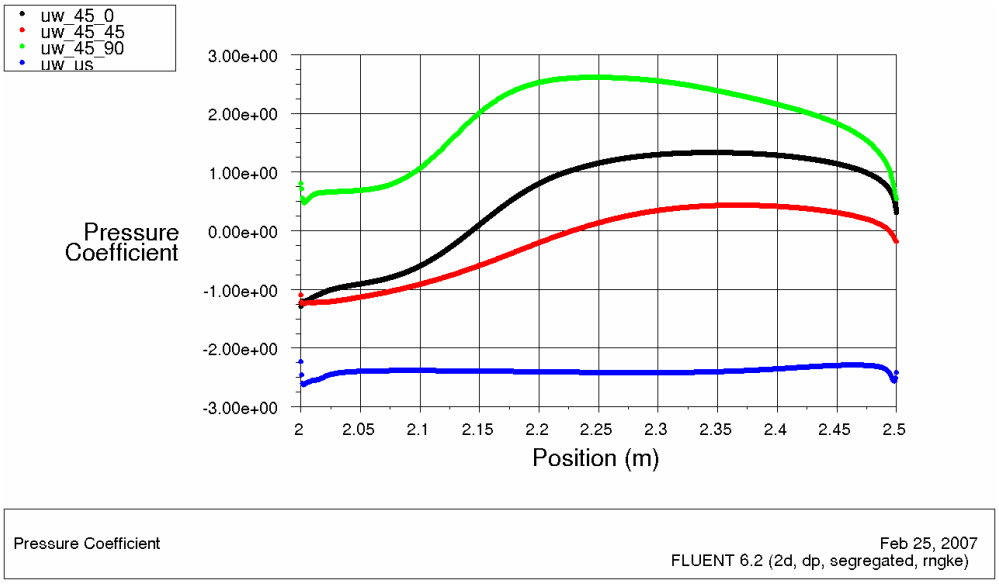

Figure 5.25: Pressure Coefficient profiles for diagonal shading devices (45_90, 45_45, 45_0) and unshaded case on upper wall

On leeward that is shown in Fig.5.26, pressure coefficient for closed case reaches maximum –1.25 and min.-2.25. On the upperwall, pressure coefficient for half-closed case reaches at a value +0.5 where is closed to the down of the windward. The minimum pressure coefficient is app. –0.75 where is closed to the upper wall intersection. The pressure coefficient for open case max value is 1.7 and min is –0.55.

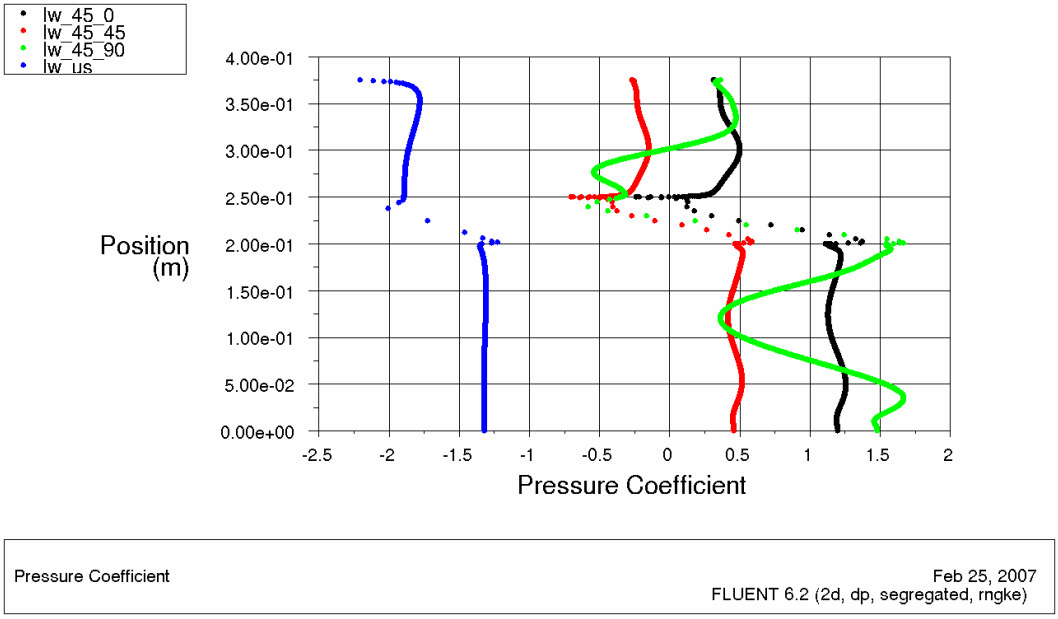

Figure 5.26: Pressure Coefficient profiles for diagonal shading devices (45_90, 45_45, 45_0) and unshaded case on upper wall

5.2.4.3 Pathlines for Diagonal Shading Devices

The pathlines for diagonal cases are analyzed in this part and drawn in Figures 5.27-; 5.30. Each figure shows separate diagonal cases airflow on the solution area and around and inside the room.

In open diagonal case, slats directed the airflow to both the upper side of the solution domain and the inner side of the room whih is shown in Figure 5.27 in general and detailed. In general view, there seems only two main vortexes ehere are inside the room and leeward. In detailed figure, there seems also a vortex on the upper wall. The main deifference for diagonal cases are the vortexes between the slats. These vortexes prevent the airflow to the inside like a closed case but let the daylighting to the inside.

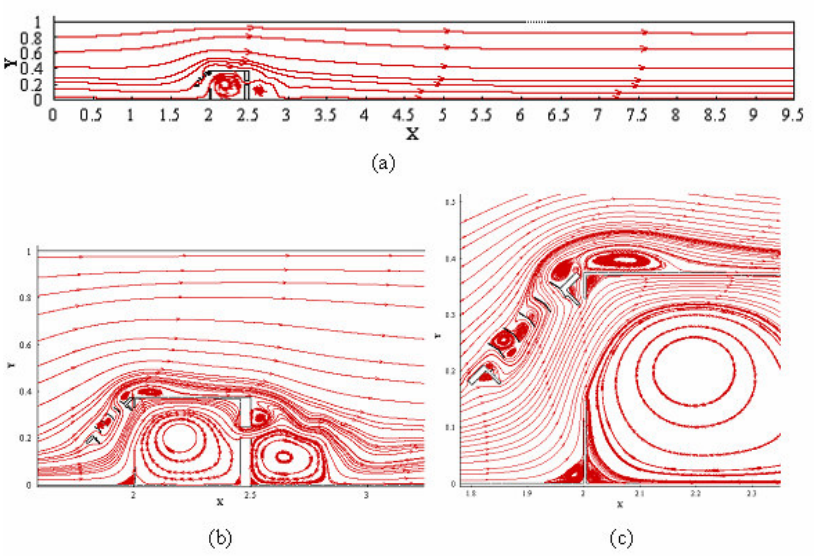

Figure 5.27: Pathlines for open diagonal shading devices (45_90) and unshadedcase a) total area b) x=1.7-3.25 c) x= 1.8-2.35

In half closed diagonal case behaves like open diagonal case. There are differnces in minumum scale like the shape of height of the room inside bubble and and the location of the bubbles between the slats. There also an airflow between the slats and it helps the daylighting.

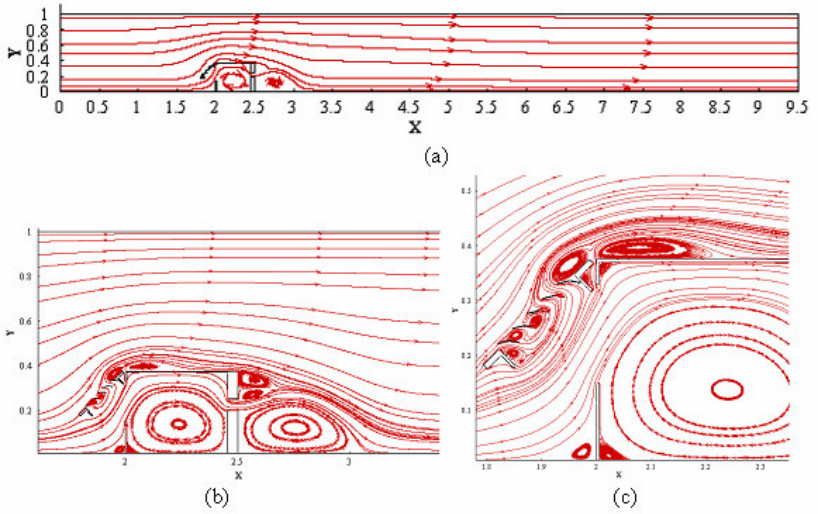

Figure 5.28: Pathlines for halfopen diagonal shading devices (45_90) and unshaded case a) total area b) x=1.7-3.25 c) x= 1.8-2.35

As it is seen in Figure 5.29, the closed diagonal shading devices has two main vortexes where are inside the room and leeward wall. The deatiled figures showas that there also occurs a vortex on the upper wall. The shear layer vortex is

minimized.The closed slats direcst the flow in to the room smoothly. There is no extra bubbles around the slats. As a result of this, the upper wall vortex is the smallest in diagonal shadin devices.

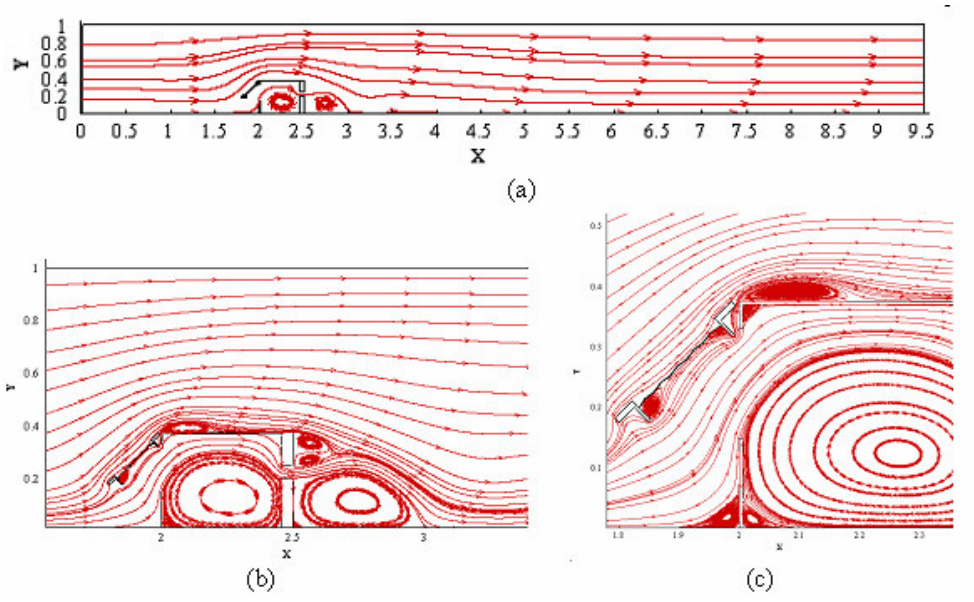

Figure 5.29: Pathlines for closed shading devices (45_0) and unshaded case a) total area b) x=1.7-3.25 c) x= 1.8-2.35

Figure 5.30 summarizes the diagonal shading devices' airflow movement. As a summary, open and half open cases has vortexes between the slats. As a result of these, the two cases behaves like closed case but in daylighting point it differs and is relatively an advantage. The slat vortexes cause an enlargement on the upper wall vortexes.

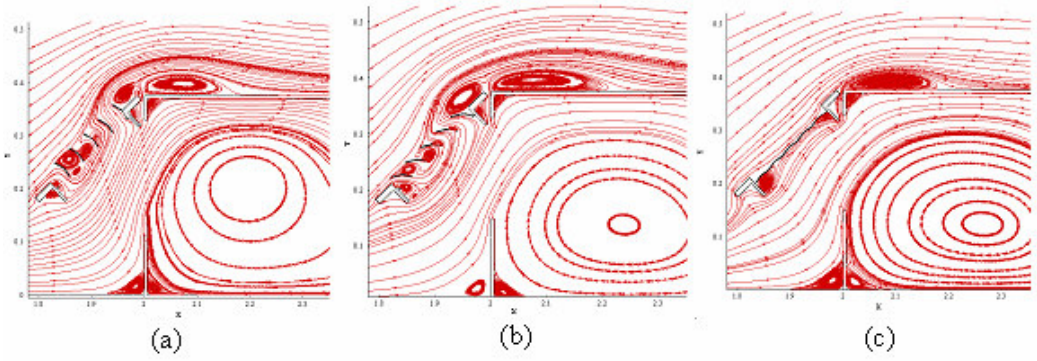

Figure 5.30: Pathline comparison between three diagonal cases a) 45_90 b) 45_45 c) 45_0

5.3 Summary

In this study, ten different case studies are discussed which are, one unshaded, three horizontal shading devices, three vertical shading devices, and diagonal shading devices. Velocity profiles in the centre of the room, pressure coefficients on the windward, upper wall, and leeward, and finally pathlines of each case are shown in figures.

Table 5.3 is summarized the velocities at x=4.5h and y=0.3h to discuss the ventilation side. This point is taken to show results depending on the assumption that a working person height will be at this point when he/she is working on a table. At comfort levels, normally the velocity inside the room should be lower than 0.5 m/s. Only unshaded, vertical closed and diagonal half closed cases are satisfied this condition. Especially, horizontal closed case has a high velocity at this point which is 1.75m/s (6.3km/h) since the shading devices behaves as an upper wall and directed all the airflow through the room, there is no leakage.

Vertical closed case seems the best situation at the point of view ventilation, velocity at the workers level is 0.3 m/s. When we consider the day lighting issue, there is no lighting gain through the window to the room because of the closed slats.

Table 5.3: Velocities for all cases at x=4.5h and y=0.3h

Case		Velocity at x=4.5h, y=0.3h
Unshaded		0.3
Horizontal_closed	(90_0)	1.75
Horizontal_halfclosed	(90_45)	0.5
Horizontal_open	(90_90)	0.9
Vertical_closed	(0_0)	0.3
Vertical_halfclosed	(0_45)	0.9
Vertical_open	(0_90)	0.5
Diagonal_closed	(45_0)	0.7
Diagonal_halfclosed	(45_45)	0.4
Diagonal_open	(45_90)	1.3

The best decision about the selection of the shading devices can be decided considering the heat management and the 3D CFD solutions. Because of the buoyancy effects, the natural ventilation speed would affect in real life, there also

occurs extra forces and loses depending on the third dimension. This study can be used as a baseline for 3D simulations and energy coupled solutions.

Table5.4: Maximum and minimum pressure coefficients for all cases

Case	Cd windward		Cd upperwall		Cd leeward	
	Max	Min	Max	Min	Max	Min
Unshaded	+2.3	-1.5	-2.27	-2.6	-1.3	-2.2
Horizontal_closed (90_0)	27	9.5	12	9	11	7.5
Horizontal_halfclosed (90_45)	5	-2	0.5	-1	1	-1
Horizontal_open (90_90)	4	-3	1.95	-1.5	-1.2	-2.2
Vertical_closed (0_0)	5.8	-3	0.7	-2.4	-0.2	-3.5
Vertical_halfclosed (0_45)	7	-1.3	1.5	-0.25	1.8	-0.1
Vertical_open (0_90)	3	-3	0.5	-2.25	-0.2	-0.8
Diagonal_closed (45_0)	2	-2	-2.2	-2.6	-1.25	-2.25
Diagonal_halfclosed (45_45)	8.5	-0.5	0.5	-1.2	0.5	-0.75
Diagonal_open (45_90)	4.2	-1.6	1.4	-1.3	1.7	-0.55

Table 5.4 is a short review of the pressure coefficients for all cases. It is practical way to compare all studies Cps on windward, upper wall and leeward. Maximum pressure coefficient occurs on horizontal closed case for all three walls because of the shading device. Horizontal closed shading device behaves like wall and forced directed the airflow to the room. This action raised extra forces on the room walls' and this causes an increase on the pressure coefficient. This case also seems a problem at the view of daylighting. It has a positive gain in daylighting when we compare it with the case vertical closed. The best results and comments can be done after applying a simulation on daylighting

.

6. CONCLUSION

In the present work the effects of wind differences on the natural ventilation is introduced. Exterior shading devices used as a tool for controlling the wind effects inside the buildings. The slat angles and positions of the shading devices affect the airflow mechanisms and the natural ventilation of the buildings.

Energy issue has become a key concern because of the environmental and economic reasons among the countries all around the world. Countries are searching ways to reduce the energy consumption in order to ensure global energy sustainability. Buildings are significant energy consumers and have an important role on the energy context so that they have a priority in the many countries policies.

Saving energy is the most cost effective way to meet our future energy needs and to prevent the air pollution for the indoor and outdoor environment. Buildings have a high potential for energy savings. Many Governments around the world are enhancing their building energy codes aiming to limit the energy consumption at a minimum level possible. In order to ensure the energy limitations, the energy consumption level of a building should be tried to keep at a minimum.

As an effective way to succeed energy consumption is natural ventilation. The cross ventilation inside the buildings lowers the energy needing for cooling. The shading devices especially used in tropical climates. The position of the shading devices and various slat angles affect the natural ventilation.

The pressure disturbances caused by wind and buoyancy is an effective way to optimize the natural ventilation. Using shading devices the wind effect could be controlled on the building facade.

Computational or wind tunnel model could be used for utilizing the best shading device position and slat angle. Wind tunnels are limited with the flexibility of the

model, labor costs and model costs. In CFD method, it has a wide range of model description to choose the best way. Comparing with the wind tunnel model, it has only computational costs. In this research, GAMBIT / FLUENT which is a commercial CFD package is used for analyzing the air change phenomena of inside and around the building and the shading devices.

The results of the case studies, horizontal (open, half_closed, closed), vertical (open, half_closed, closed), and diagonal (open, half_closed, closed) shows that the vertical shading devices lowered the airflow of building inside.

For the future work, the boundary conditions for the computational solution could be modified for the real conditions (wind velocity, natural conditions etc.). An algorithm could be written to define the wind velocity and ABL. The radiation models and energy equations could be solved and the solar gains for model could be calculated.

Furthermore, the model could be defined and solved in 3-D and not only horizontal slats solved but also vertical slats can be analyzed. A compact relation between wind tunnel experiments and computational model can be sustained.

In addition to this, daylighting effects of shading devices could be considered and included into the solution area.

7. REFERENCES

Allard F., 1998, Natural Ventilation in Buildings: A Design Handbook, James& James Ltd, London.

Blazek, J., 2001, Computational Fluid Dynamics: Principles and Applications, Elsevier, London.

Bottema, M., 1980, Wind climate and urban geometry, Ph.D. Thesis, Eindhoven University of Technology, Eindhoven, The Netherlands.

BSI, 1991, Code of Practice for ventilation principles and designing for natural ventilation, British Standard, BS5925.

Chen, Q., 1995, Comparison of different k-e models for indoor air flow computations, Numerical Heat Transfer, Part B- Fundamentals 28(3): 353-369.

Chen, Q., 2004, Using computational tools to factor wind into architectural environment design, Energy and Buildings(in press).

Chen, Q. and Xu, W., 1998, A zero-equation turbulence model for indoor airflow simulation, Energy and Buildings 28:137-144.

CIBSE AM10, 1997, Natural ventilation in non-domestic buildings, Chartered Institute of Building Services Engineers, Application Manual.

CIBSEAM Briefing8, 2003, Reducing emissions through energy efficiency-key issues to edress in designing and operating buildings.The Chartered Institution of Building Services Engineering. London.

Cook, M. J., Ji, Y., and Hunt, G.R., 2003, CFD modelling of natural ventilation: combined wind and buoyancy forces, International Journal of Ventilation1 (3): 169-179.

Cook, N.J., 1985, The designer's guide to wind loading of building structures-Part1: Background, damage survey, wind data and structural classification. Butterworths, London, UK.

Desam, **P.R.**, 2003, Cfd_Fluent Lecture Notes, University of Utah.

Etheridge, D.W., 2000, Unsteady flow effects due to fluctuating wind pressures in natural ventilation design-mean flow rates, Building and Environment 35(2):11-133.

Fluent , 2006, Fluent version 6.2 user's manual.
URL: www.fluent.com/software/fluent /index.htm

Gan, G., 1999, Lectures Notes-Building Ventilation, Msc course in Renewable Energy and Architecture, University Nottingham.

Heiselberg, P., 1999, The hybrid ventilation process- theoretical and experimental work, Air Infiltration Review 21(1).

Hunt, G.R. and Linden, P.F., 1999, The fluid mechanics of natural ventilation-displacement ventilation by buyocancy-driven flows assisted by wind, Building and Environment 34(6):707-720.

Jiang, Y.D., Alexander, H., Jenkins, Arthur, R., and Chen, Q., 2003, Natural ventilation in buildings: measurement in a wind tunnel and numerical simulation with large-eddy simulation, Journal of Wind Engineering and Industrial Aerodynamics 91(3): 331-353.

Launder, B.E., Spalding D.B., 1974, The numerical computation of turbulent flows, Computer Methods in Applied Mechanics and Engineering 3: 269-289.

Lechner N., 2000, Heating, Cooling, Lighting: Design Methods for Architects, 2nd ed., John Wiley & Sons, Inc.

Liddament, M. W., 1991, A review of building air flow simulation, AIVC Technical Note 33, Air Infiltration and Ventilation Centre, Coventry, UK.

URL: www.aivc.org/Publications/Technical_reports/TN33.html

Li,Y., Delsante, A., Symons, J.G., Chen, L., 1998, Comparison of zonal and CFD modelling of natural ventilation Centre in a thermally stratified building., 6th International Conference on Air Distribution in Rooms-Roomvent 98, Stockholm, Sweden.

Nishizawa, S.T., Sawachi, T., Narita, K., Seto, H. And Ishikawa,Y., 2003, A wind tunnel sull scale building model comparison between experimental and CFD results based on the standard k-e turbulence representation. International Journal of Ventilation 2(4): 419-429.

Ok,V., Turkmenoglu, N., 2005, Investigation of the effects of the solar control elements on interior air movements, Unpublished doctoral dissertation, ITU, İstanbul.

Straw, M.P., 2000, Computation and measurements of wind induced ventilation, PhD thesis. University of Nottingham, UK.

URL: www.nottingham.ac.uk/~evzngw/download.html

Tennekes, H. and Lumley, J., 1972,A First Course in Turbulence. The MIT Press, Cambridge, Massachusetts.

Tomoyuki, E., Kurabuchi ,T., Ishii, M., Komamura, K., Maruta, E., and Sawachi,T., Study on the Numerical Predictive Accuracy of Wind Pressure Distribution and Air Flow Characteristics, International Journal of Ventilation, Volume4.

Versteeg, H.K., Malalasekara, W., 1995, Introduction to computational fluid dynamics, the finite volume method. Longman Scientific & Technical, Harlow.

URL: www.wind.ttu.edu

APPENDIX A

The solver definitions of Unshaded case
FLUENT
Version: 2d, dp, segregated, rngke (2d, double precision, segregated, RNG k-epsilon)
Release: 6.2.16
Title: Unshaded - fine mesh
Models

Model	Settings
Space	2D
Time	Steady
Viscous	RNG k-epsilon turbulence model
Wall Treatment	Enhanced Wall Treatment Functions
RNG Differential Viscosity Model	Disabled
RNG Swirl Dominated Flow Option	Disabled
Heat Transfer	Disabled
Solidification and Melting	Disabled
Species Transport	Disabled
Coupled Dispersed Phase	Disabled
Pollutants	Disabled
Soot	Disabled

Solver Controls

Equations

Equation	Solved
Flow	yes
Turbulence	yes

Numerics

Numeric	Enabled
Absolute Velocity Formulation	yes

Relaxation

Variable	Relaxation Factor
Pressure	0.2
Density	1
Body Forces	1
Momentum	0.4
Turbulence Kinetic Energy	0.4
Turbulence Dissipation Rate	0.4
Turbulent Viscosity	0.5

Linear Solver

Variable	Solver Type	Termination Criterion	Residual Reduction Tolerance
Pressure	V-Cycle	0.1	
X-Momentum	Flexible	0.1	0.7
Y-Momentum	Flexible	0.1	0.7
Turbulence Kinetic Energy	Flexible	0.1	0.7
Turbulence Dissipation Rate	Flexible	0.1	0.7

Discretization Scheme

Variable	Scheme
Pressure	Second Order
Momentum	Second Order Upwind
Turbulence Kinetic Energy	Second Order Upwind
Turbulence Dissipation Rate	Second Order Upwind

Solution Limits

Quantity	Limit
Minimum Absolute Pressure	1
Maximum Absolute Pressure	5e+10
Minimum Temperature	1
Maximum Temperature	5000
Minimum Turb. Kinetic Energy	1e-14
Minimum Turb. Dissipation Rate	1e-20
Maximum Turb. Viscosity Ratio	100000

RESUME

She was born in Kocaeli in 1980. She finished Oruc Reis Anatolian High School in Kocaeli. She graduated from Istanbul Technical University as Mechanical Engineer in 2003. She started her master's degree in Mechanical Engineering department Thermo-Fluid Program in ITU. She studied in Stuttgart University of Applied Sciences (SAS) in 2004 in the framework of Erasmus Exchange Program. She worked in SAS as research assistant between March 2006 and January 2007.